Chem Soc Rev

Zeolitic imidazolate framework composite membranes and thin films: Synthesis and applications

Journal:	*Chemical Society Reviews*
Manuscript ID:	CS-REV-12-2013-060480.R1
Article Type:	Review Article
Date Submitted by the Author:	06-Feb-2014
Complete List of Authors:	Yao, Jianfeng; Monash University, Department of Chemical Engineering Wang, Huanting; Monash University, Department of Chemical Engineering

SCHOLARONE™
Manuscripts

Cite this: DOI: 10.1039/c0xx00000x

www.rsc.org/xxxxxx

ARTICLE TYPE

Zeolitic imidazolate framework composite membranes and thin films: Synthesis and applications

Jianfeng Yao* and Huanting Wang*

Received (in XXX, XXX) Xth XXXXXXXXX 20XX, Accepted Xth XXXXXXXXX 20XX

DOI: 10.1039/b000000x

Zeolitic imidazolate frameworks (ZIFs), a subclass of metal organic frameworks, are built of tetrahedral metal ions bridged by imidazolates. They have permanent porosity and relatively high thermal and chemical stability, which make them attractive candidates for many industrial applications. In recent years, significant progress has been made in developing ZIFs into membranes and thin films for gas separation, liquid separation (pervaporation) and functional devices. Various techniques, such as direct synthesis, secondary synthesis, reactive seeding and functional chemicals as linkers, and contra-diffusion synthesis, have been reported for the fabrication of ZIF membranes and films. As ZIFs have good compatibility with polymers, they have been incorporated into polymers with high loadings to form mixed matrix membranes. The resulting symmetric dense or asymmetric composite membranes exhibit good performance in gas separation and liquid separation via pervaporation. The recent developments of ZIF membranes/films, ZIF/polymer mixed matrix membranes and their applications are reviewed in this article.

1. Introduction

Zeolitic imidazolate frameworks (ZIFs) are a class of porous crystals with extended three-dimensional structures constructed from tetrahedral metal ions (e.g., Zn, Co) bridged by imidazolate (Im). The fact that the M-Im-M angle is similar to the Si-O-Si angle (145°) preferred in zeolites has led to the synthesis of a large number of ZIFs with zeolite-type tetrahedral topologies.[1,2] Remarkably, ZIFs exhibit permanent porosity and high thermal and chemical stability, which make them attractive candidates for many applications such as adsorption, separation and gas storage. ZIFs are a subclass of metal organic frameworks (MOFs, also known as porous coordination polymers),[3] which have been extensively studied over the last 15 years.[3,4] In particular, the processing of MOFs into membranes and films is important for many applications, such as separation membranes and chemical sensors.[5] The techniques for the fabrication of MOF membranes and films mainly translate from the two closely related fields: (1) zeolite films, particularly the direct synthesis and secondary growth methods, and (2) coordination polymer films with Langmuir-Blodgett and layer-by-layer thin-film preparation techniques on which the literature is abundant.[6,7] In recent years, MOF membranes and films have been intensively studied, and several excellent reviews have been published,[5,8-12] where ZIF membranes and films were partially discussed.

In comparison to the other MOFs, ZIFs share many riches of zeolite chemistry, both in structural topologies and in coordination factors, and show exceptional thermal and chemical stability.[13,14] Therefore, ZIFs hold much great promise as porous materials for a variety of applications. In this review, we only focus on the synthesis and applications of ZIF membranes and films, and the mixed matrix membranes incorporated with ZIFs for gas separation, pervaporation, and functional devices, although the synthesis methods and applications presented here may be applicable to other MOFs. The first literature for the synthesis of ZIF crystals was published in 2003[15] and the ZIF membranes have rapidly emerged since 2010. This review is organized as the following sections: 1) Introduction; 2) Synthesis of ZIF separation membranes for gas separation and pervaporation; 3) ZIF/polymer mixed matrix membranes; 4) ZIF films for microelectronics; and 5) Conclusions and perspectives. The synthesis and applications of ZIF composite membranes and films are summarized in Scheme 1.

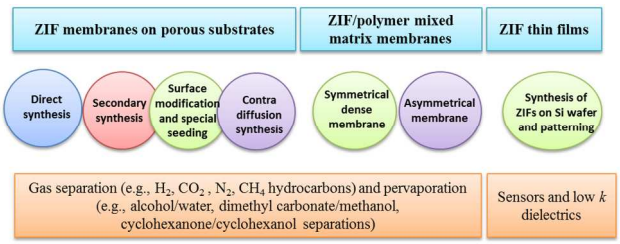

Scheme 1. Summary of the synthesis and applications of ZIF composite membranes and films.

2. Synthesis of ZIF separation membranes for gas separation and pervaporation

The well-defined porous structures of ZIFs allow them to achieve gas separation with high selectivity due to the molecular sieving

effect.[16] Table 1 summarizes the porous structures of ZIFs discussed in this review. The pore size of ZIFs is usually less than 5 Å, which is in the range of small molecular gases and liquids. Due to the versatility of imidazolate linkers, the pore size and surface property of ZIFs could be adjusted by using different (functionalized) linkers. Therefore, considerable efforts have been made to develop ZIF membranes for gas separations such as hydrogen purification, CO_2 capture, natural gas purification, light hydrocarbon separation, and for liquid separation via pervaporation.

Like zeolite membranes, ZIF membranes are prepared by growing a thin ZIF layer on porous substrates such as porous ceramic and stainless steel discs and tubes, and porous polymer sheets. The porous substrates provide mechanical support for ZIF layer, and exhibit minimal permeation resistance. The quality and nature of the substrates, such as surface roughness, pore size and chemical composition, has a significant effect on the formation of ZIF layer. The main task for the synthesis of high-quality ZIF membranes is to control ZIF heterogeneous nucleation and crystallization on the substrate surface, and minimize intercrystal voids. The quality of ZIF membranes is evaluated in terms of crystal structure and morphology and separation properties. In particular, the gas separation properties of the membranes are determined by using single gas and mixed gas permeation experiments.[8-10,17-19]

The permeance P_i (mol m^{-2} s^{-1} pa^{-1}) of single gas *i* (or component *i* in the mixed gas feed) is defined as

$$P_i = \frac{N_i}{\Delta p_i A}$$

where N_i is the permeating flow rate of single gas (or component *i*) (mol s^{-1}), Δp_i is the transmembrane pressure difference of *i* (Pa), and A is the membrane area (m^2). Similarly, the permeance P_j can be written for single gas *j* (or component *j*). The ideal selectivity (or separation factor), S_{ij} is defined as the ratio of the two permeances P_i and P_j.

$$S_{ij} = \frac{P_i}{P_j}$$

ZIF composite membranes have been studied for liquid separation via pervaporation. Pervaporation is considered as one of the most promising technologies in the molecular-scale liquid/liquid separations for biorefinery, petrochemical and pharmaceutical industries.[20] When a mixed liquid stream containing two or more components is placed in contact with one side of the membrane, the components will absorb into/onto the membrane. The penetrants will diffuse through the membrane and evaporate as permeate induced by vacuum or gas purge. The separation of different components is achieved when some of the components preferentially diffuse across the membrane. The flux of a component i through a membrane can be expressed in terms of the partial vapor pressures on either side of the membrane, p_{io} and p_{ii}, by

$$Ji = \frac{P_i^G}{l}(p_{io} - p_{ii})$$

where J_i is the flux, l is the membrane thickness and P_i^G is the gas separation permeability coefficient. A similar equation can be written for component *j* in the feed. The separation achieved by a pervaporation membrane is proportional to the fluxes J_i and J_j through the membrane.[21]

The techniques for the synthesis of ZIF membranes can be roughly classed as direct synthesis, secondary growth, surface functionalization and special seeding, and contra-diffusion (counter-diffusion) for convenience of discussion. The synthesis processes and the properties of ZIF membranes are reviewed below.

Table 1. ZIFs for the preparation of membranes and films.

ZIF type	Molecular structure	Topology	Pore size (nm)	Ref.
ZIF-7	$Zn(benzimidazole)_2$	SOD	0.30	2,15
ZIF-8	$Zn(2\text{-methylimidazole})_2$	SOD	0.34	2,22
ZIF-9	$Co(benzimidazole)_2$	SOD	<0.30	2
ZIF-22	$Zn(5\text{-azabenzimidazolate})_2$	LTA	0.30	13
ZIF-69	Zn(cbIM)(nIM) nIM: 2-nitroimidazole; cbIM: 5-chlorobenzimidazole	GME	0.44	23
ZIF-71	$Zn(4,5\text{-dichloroimidazole})_2$	RHO	0.42	23
ZIF-78	Zn(nbIm)(nIm) nbIm: 5-nitrobenzimidazole; nIm: 2-nitroimidazole	GME	0.38	24
ZIF-90	$Zn(imidazolate\text{-}2\text{-}carboxyaldehyde)_2$	SOD	0.35	25
ZIF-95	$Zn(5\text{-chlorobenzimidazole})_2$	POZ	0.37	26
SIM-1	Zn (4-methyl-5-imidazolecarboxaldehyde)$_2$	SOD	<0.34	27
ZIF-9-67	Co(benzimidazole)(2-methylimidazole)	SOD	<0.34	28

2.1. Direct synthesis

In the direct synthesis, a porous membrane substrate without surface modification is immersed in a ZIF synthesis solution, where a ZIF layer directly grows on the substrate. Many different types of ZIF membranes have been successfully synthesized using this method. For instance, as the promising porous materials, ZIF-8 membrane is able to separate H_2 (its kinetic diameter ~2.9 Å) from larger molecules as the pore size of ZIF-8 is ~3.4 Å. Another important feature of ZIF-8 is its hydrophobic nature, whereas ultramicroporous zeolites are usually hydrophilic. This should give ZIF-8 membrane an advantage over zeolites in the separation of H_2 from a mixture with water vapor. Bux et al. prepared ZIF-8 membrane on titania support by microwave-assisted solvothermal synthesis.[29] A cleaned and dried support was firstly immersed into the precursor and left standing for 20 min. Afterwards the solution with the support was transferred into a 200 ml Teflon autoclave and heated in a microwave oven to 100 °C for 4 h to complete the membrane preparation. The resulting membrane is about 30 μm in thickness (Fig. 1), and the single gas permeation test showed the permeances clearly depend on the molecular size of the gases (Fig. 1). The single gas separation performance of various ZIFs is summarized in Table 2. The separation factor for a 1:1 H_2/CH_4 mixture at 298 K and 1 bar was determined to be 11.2, which considerably exceeds the Knudsen separation factor for H_2/CH_4 (~2.8). The permeation selectivity of CO_2/CH_4 could be predicted by IR-diffusion studies and molecular modelling, and the results fitted the experimentally measured permeation selectivities.[29,30] ZIF-8 was predicted by Haldoupis et al. to have extraordinarily high membrane

This journal is © The Royal Society of Chemistry [year]

selectivity for CO_2/CH_4 mixtures in theoretical calculations based on a rigid crystal structure.[31] Furthermore, the ethene/ethane separation by ZIF-8 membrane was also estimated with sufficient accuracy by using the adsorption and diffusion selectivity on a ZIF-8 large single crystal by IR microscopy. ZIF-8 membrane showed ethene/ethane separation factors of 2.8 and 2.4 at room temperature for 1 and 6 bar feed pressure, respectively.[32]

The role of sodium formate was investigated to the synthesis of ZIF-8 membrane. A one step *in situ* synthesis of ZIF-8 membranes on unmodified porous α-alumina supports was developed in the presence of sodium formate. Sodium formate was found to enhance the heterogeneous nucleation of ZIF-8 crystals on alumina supports as well as to promote intergrowth of ZIF-8 crystals. In this *in situ* method, sodium formate played a critical role in formation of well-intergrown continuous ZIF-8 membranes, and the ideal selectivity of H_2/N_2 increased to 12.0 with a H_2 permeance of 2.4×10^{-7} mol m^{-2} s^{-1} pa^{-1}.[33] A substituted imidazolate-based ZIF (SIM-1) membrane was also crystallized *in situ* on a tubular asymmetric alumina support.[27] SIM-1 has the same SOD topological structure as ZIF-8 with 4-methyl-5-imidazolecarboxaldehyde as the imidazolate linker. The size and the shape of the functionalized imidazolate linker make the SOD cavity much smaller in SIM-1. The thickness of the resulting SIM-1 membrane was ca. 25 μm. The H_2/N_2 ideal selectivity of 2.5 was obtained, which was smaller than its Knudsen selectivity (3.7); its CO_2/N_2 selectivity (1.1) was slightly greater than the corresponding Knudsen selectivity (0.78), thus indicating an adsorption-diffusion based mechanism. For a ternary mixture $CO_2/N_2/H_2O$ (10/87/3 vol%), a CO_2/N_2 separation factor of 4.5 was measured, which is much higher than the corresponding Knudsen separation factor (0.78).[27]

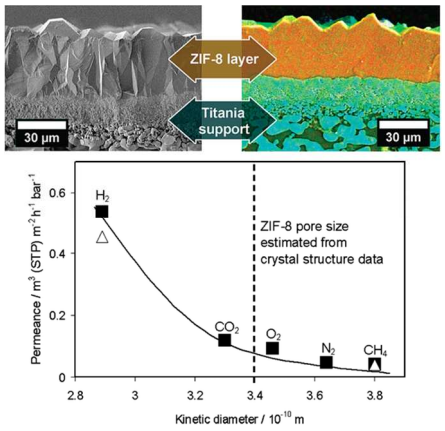

Fig. 1. SEM image and EDXS mapping of the cross section of a simply broken ZIF-8 membrane, and Single (squares) and mixed (triangles) gas permeances for a ZIF-8 membrane vs kinetic diameters. Adapted with permission from ref. 29. Copyright 2009 American Chemical Society.

ZIF-69 is composed of zinc nitrate coordinated with 2-nitroimidazole (nIM) and 5-chlorobenzimidazole (cbIM), forming a zeolite GME topology that has 12-membered ring (MR) straight channels along the c-axis and 8 MR channels along the a- and b-axes.[23] Continuous and *c*-oriented ZIF-69 membranes were successfully synthesized on porous α-alumina substrates with a thickness of ca. 50 μm by an *in situ* solvothermal method. Single-gas permeation experiments through ZIF-69 membranes were carried out by the vacuum permeation method at room temperature using H_2, CH_4, CO, CO_2 and SF_6, respectively. The permeances were in the order of H_2 >CO_2 >CH_4 >CO>SF_6. The separation of CO_2/CO gas mixture was investigated by gas chromatography and the permselectivity (or separation factor) of CO_2/CO was 3.5 with CO_2 permeance of 3.6×10^{-8} mol m^{-2} s^{-1} pa^{-1} at room temperature.[34]

Many ZIF membranes have been synthesized using the direct synthesis method so far. Given that the crystallization depends on many factors, it is often difficult to control ZIF crystallization on unmodified substrate, resulting in defective ZIF membranes with many intercrystal voids. To improve the quality of ZIF membranes, secondary growth and other new techniques are usually required.

2.2. Secondary growth

Secondary growth, also called seeded growth, is more commonly used in the membrane preparation.[7] In this synthesis process, ZIF crystals are synthesized first and deposited on substrates using different methods such as dip coating and rubbing of dry ZIF powder. The ZIF crystals deposited on the substrate serve as seeds for promoting ZIF crystallization. Secondary growth allows for more effective control of crystal growth and orientation of ZIF membranes.

Thin ZIF-8 membranes with ~5-9 μm thicknesses were synthesized by secondary seeded growth on tubular α-alumina supports. The separation performance of these membranes for equimolar CO_2/CH_4 gas mixtures was demonstrated. The membranes displayed CO_2 permeances as high as ca. 2.4×10^{-5} mol m^{-2} s^{-1} Pa^{-1} with CO_2/CH_4 separation selectivities of 4.1-7.0 at 295 K and a feed pressure of 139.5 KPa.[35] Bux et al. prepared highly oriented ZIF-8 composite membranes by seeding and secondary growth.[36] By dip-coating, ZIF-8 nanocrystals were attached onto the surface of a porous α-alumina support using polyethyleneimine (PEI) as a coupling agent. The membrane showed preferred orientation of the {100} plane parallel to the support (Fig. 2). The crystallographic preferred orientation (CPO)[37] indices of the dominant 200 reflection in relation to the 110 ($CPO_{200/110}$) and the 211 reflections ($CPO_{200/211}$) were calculated to be 83 and 81, respectively. Both values clearly demonstrated the pronounced {100} orientation with only a low fraction of crystals taking different orientations. In binary gas permeation experiments, the membrane showed good performance in H_2/hydrocarbon separation. A sharp molecular sieve separation was observed for an equimolar H_2/C_3H_8 mixture with a separation factor above 300.[36] The addition of PEI in the seeding solution could improve the adhesion between the seed crystals and the support surface.[38]

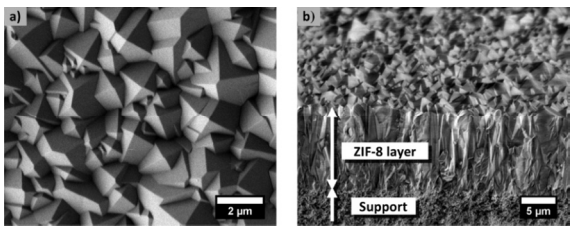

Fig. 2. (a) SEM top view of the well-intergrown ZIF-8 layer after 2 h of secondary growth. (b) SEM top down view on the corresponding crosssection of the broken membrane. Reprinted with permission from ref. 36. Copyright 2011 American Chemical Society.

Exceptionally high quality ZIF-8 membranes were prepared in aqueous solutions at near room temperature, which is more economical and greener compared to other synthesis procedures requiring organic solvents and high synthesis temperature. The membrane thickness was around 2.5 μm, and exhibited excellent separation performance for C2/C3 hydrocarbon mixtures. The separation factors for mixtures of ethane/propane, ethylene/propylene and ethylene/propane are ~80, ~10 and ~167, respectively.[39] For the propylene/propane binary mixture separation, the ZIF-8 membrane showed a permeability of propylene up to ca. 3.0×10^{-8} mol m^{-2} s^{-1} pa^{-1} and a propylene to propane separation factor up to 50 at optimal separation conditions, well surpassing the "upper-bound trade-off" lines of existing polymer and carbon membranes.[40] The diffusivity value of the high quality ZIF-8 membrane decreased with increasing molecular size in the order He>H_2>CO_2>N_2>CH_4.[41] Gas permeance for the above light gases remained constant while C_3H_6 and C_3H_8 permeance decreased with increasing pressure due to the specific pressure dependency of the adsorption isotherm for each gas. The determined diffusivity for propylene and propane is 1.25×10^{-8} and 3.99×10^{-10} cm^2/s with respective activation diffusion energy of 12.7 and 38.8 kJ/mol. With an equimolar binary feed, the ZIF-8 membranes exhibited a consistent C_3H_6/C_3H_8 selectivity of about 30 and a C_3H_6 permeance of 1.1×10^{-8} mol m^{-2} s^{-1} Pa^{-1}.[41] By using the secondary growth method, Yao et al. prepared continuous ZIF-8 membranes in a diluted aqueous solution with a Zn^{2+}: hmim: H_2O molar ratio of 1:70:4952, and their thicknesses were about 0.8-1.4 μm. ZIF-8 membranes and micro-sized crystals could be prepared simultaneously in such diluted aqueous solution. Gas permeation tests indicated the ZIF-8 membranes were continuous and compact.[42]

As hollow fiber membranes can be easily assembled into compact membrane modules for industrial separation processes, the development of ZIF hollow fiber membranes is desirable for practical applications. Xu et al. prepared ZIF-8 membranes on the outer surface of alumina hollow fibers from a concentrated synthesis gel by three times of solvothermal synthesis.[43] The crystalline ZIF-8 membranes were compact and continuous, and contained micro-cavities. Single gas permeances of H_2, N_2, CH_4 and CO_2 were determined as a function of permeation time at 25°C. H_2, N_2 and CH_4 permeances almost did not change with the permeation time. However, CO_2 permeance decreased from 9.8×10^{-8} to 1.7×10^{-8} mol m^{-2} s^{-1} pa^{-1} within 12 h, and CO_2 permeation led to an unrecoverable reduction in gas permeation rates in the further permeation experiments. After the first round tests, H_2, N_2, CH_4 and CO_2 permeances in the second round permeation tests dropped by 40%, 24%, 11%, and 6%, and remained constant in the further repeated measurements; the ideal selectivities of H_2/CO_2, N_2/CO_2 and CH_4/CO_2 were 32.2, 12.9, and 11.9, respectively. For a H_2/CO_2 binary mixture (45% H_2), the H_2/CO_2 separation factor was 7.1. The small CO_2 permeance should arise from strong CO_2 adsorption in ZIF-8 membranes with micro-cavities, and the adsorbed CO_2 partially blocked the gas permeation.[43] Such membranes may be further explored for CO_2 related separation applications. By a crystallizing-rubbing seed deposition and secondary growth, a continuous well-intergrown ZIF-8 membrane on hollow ceramic fiber tube was synthesized. The obtained ZIF-8 membrane was compact and continuous, with a thickness of about 5 μm. The membrane displayed high H_2 molecular sieve separation performance. Specifically, the H_2 permeance reached an excellent value of 1.1×10^{-6} mol m^{-2} s^{-1} pa^{-1}, and the ideal separation factors for H_2/CO_2, H_2/N_2 and H_2/CH_4 were calculated to be 5.2, 7.3 and 6.8 at room temperature, respectively.[44] Pan et al. prepared yttria-stabilized zirconia (YSZ) hollow fiber-supported ZIF-8 membranes by using a mild and environmentally friendly seeded growth method in aqueous solution. Single gas permeation studies demonstrated that the membrane had a very high hydrogen permeance (1.54×10^{-6} mol m^{-2} s^{-1} pa^{-1}) and an ideal selectivity of H_2/C_3H_8 of more than 1000 at room temperature (Fig. 3).[45]

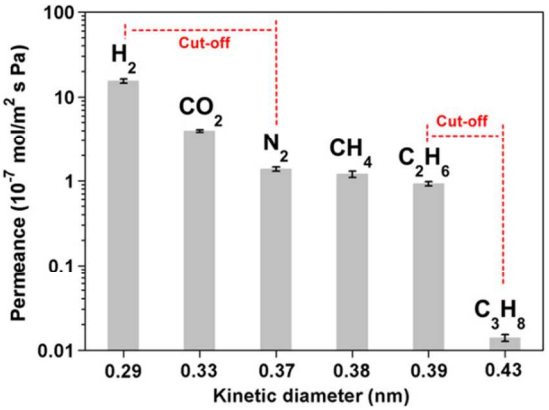

Fig. 3. The permeation of single gases through ZIF-8 membrane in relation to the kinetic diameters of the gases measured at room temperature. Reprinted with permission from ref. 45. Copyright 2012 Elsevier.

ZIF-7 ($Zn(bim)_2$) is formed by bridging benzimidazolate (bim) anions and zinc cations with sodalite (SOD) topology.[2,15] The pore size of ZIF-7 (the hexagonal window size in the SOD cage) estimated from crystallographic data is about 0.3 nm, which is just in between the size of H_2 (0.29 nm) and CO_2 (0.33 nm). ZIF-7 membrane was prepared by a seeded secondary growth method.[46] The synthesized ZIF-7 nanoseeds could be dispersed in methanol or *N*,*N*-dimethylformamide (DMF) to form stable colloidal dispersions. When these colloidal dispersions were used to seed alumina supports, however, the seed layer easily came off the supports. To address this problem, Li et al. dispersed the ZIF-7 nanoseeds in a polyethyleneimine (PEI) solution to obtain a viscous seeding solution (containing 4 wt% ZIF-7 and 2 wt% PEI).[46] The resulting ZIF-7 membrane was activated at 200 °C for around 40 h, and the H_2 permeance reached a plateau value of approximately to 8×10^{-8} mol m^{-2} s^{-1} Pa^{-1} and the H_2/N_2 separation factor was 7.7. Fig. 4 gives the permeances of single H_2, CO_2, N_2, and CH_4 gases and from their 1:1 mixtures through the ZIF-7 membrane as a function of the kinetic diameter of the gas molecules. For both single- and mixed-gas permeation, there is a clear cut-off between H_2 and CO_2. The H_2/CO_2 ideal selectivity and separation factor are 6.7 and 6.5, respectively, which exceed the Knudsen separation factor (ca. 4.7). Nevertheless, the H_2/CO_2 separation performance exceeded the latest Robeson's "upper-bound" line.[47] The H_2/N_2 and H_2/CH_4 separation factors are 7.7 and 5.9, respectively (at 200 °C and 1 bar), both are higher than the corresponding Knudsen separation

This journal is © The Royal Society of Chemistry [year]

factors (3.7 and 2.8, respectively).[46] Due to its hydrophobicity, the ZIF-7 membrane also showed excellent hydrothermal stability in the presence of steam.[48] A post-modification was conducted on ZIF-7 layer supported on alumina hollow fibers, and the ideal selectivity of H_2/N_2 was increased after β-cyclodextrin modification. The post-modification of ZIF membranes may be an effective method for increasing the membrane separation performance. [49]

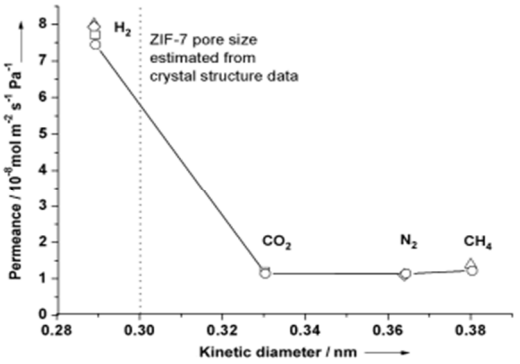

Fig. 4. Permeances of single gases (circles) and from 1:1 mixtures (squares: H_2/CO_2 mixture, rhombuses: H_2/N_2 mixture, triangles: H_2/CH_4 mixture) of the ZIF-7 membrane at 200 °C as a function of molecular kinetic diameters. Reprinted with permission from ref. 46. Copyright 2010 John Wiley & Sons, Inc.

The *c*-out-of-plane oriented ZIF-7 membrane was prepared by dip-coating and microwave assisted secondary growth.[50] ZIF-7 nanocrystals were prepared in PEI-dimethylfomamide (DMF) solution, in which the PEI was used to enhance the linkage between the seeds and the support. The resulting ZIF-7 membrane (Fig. 5) was tested for H_2/CO_2 equimolar gas mixture separation. Compared to the randomly oriented ZIF-7 membrane,[46] the oriented membrane exhibited an increase in selectivity with temperature. A H_2 /CO_2 mixture separation factor of 8.4 was measured at 200 °C,[50] which is much larger than the Knudsen separation factor of 4.7.

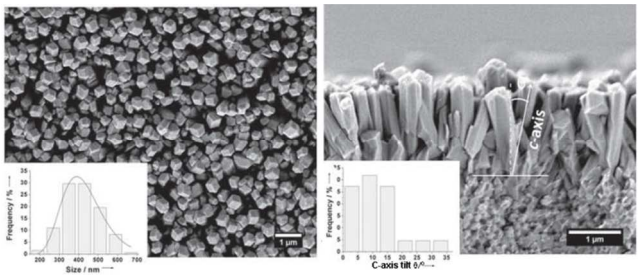

Fig. 5. SEM top views and cross sections of the ZIF-7 membranes obtained after 225 min of microwave assisted secondary growth. Insets in the SEM top views give the distributions of the cross-sectional size of the columnar crystals, and the CPO distributions. The CPO is represented by the angle θ between c axis and the substrate normal. Reprinted with permission from ref. 50. Copyright 2010 John Wiley & Sons, Inc.

The secondary growth has been shown to be more effective for controlling the crystal orientation and thickness of ZIF membrane than the direct synthesis. For instance, a highly *c*-oriented and well intergrown ZIF-69 membrane on porous α-alumina substrates was prepared by seeded secondary growth method. For the single gas permeation, the permeance of CO_2 was higher than those of N_2, CO and CH_4. The possible reason was that the permeation behavior of CO_2 was controlled by surface diffusion, which was attributed to the strong selective adsorption of ZIF-69 for CO_2.[23] The permeances of CO_2, N_2, CO and CH_4 were 23.6×10^{-9}, 10.6×10^{-9}, 8.2×10^{-9} and 8.6×10^{-9} mol m^{-2} s^{-1} Pa^{-1} at 298 K under 1 bar, respectively. The mixture-gas separation studies showed that the ZIF-69 membrane had separation factors of 6.3, 5.0, 4.6 for CO_2/N_2, CO_2/CO and CO_2/CH_4, respectively, and a permeance of ca. 1.0×10^{-7} mol m^{-2} s^{-1} pa^{-1} for CO_2 in almost all mixtures.[51] Both the separation factor and permeance were better than those of the ZIF-69 membranes prepared by the *in situ* solvothermal method [34] due to improvement in the membrane microstructure (i.e. thickness and the oriented crystal direction) by the seeded growth method.

Shekhah et al. prepared an ultra-thin and defect-free ZIF-8 membrane on alumina substrate by the liquid phase epitaxy approach (step-by-step deposition).[52,53] The thickness of the membrane was controllable in the range of ~0.5-1.6 μm with growth cycles of 150-300. The ideal selectivity obtained at 308 K was 5, 11, 12, 70 and 3.5 for H_2/CO_2, H_2/N_2, H_2/CH_4, H_2/C_3H_8, and C_3H_6/C_3H_8, respectively.[52] However, the resultant membrane fabricated by this method exhibited significantly lower gas permeance. The significant decrease in gas permeance indicated the effective fabrication of a higher quality ZIF-8 continuous membrane with minimal grain boundary micro-defects. In the equimolar gas mixture, the selectivity for C_3H_6/C_3H_8 decreased with time, reaching a steady-state value of ~2.2 after 2 days. Such a ZIF-8 membrane showed a selectivity of 4 at 308 K in the separation of 75/25 CH_4/n-C_4H_{10} gas mixture after being tested at steady state for 30 h and the selectivity was improved to ca. 16 when the temperature was raised to 323 K.[52]

Polymer-supported ZIF-8 membrane was first prepared on the porous Nylon membrane by the contra-diffusion method.[54] Good compatibilities between ZIFs and polymers were expected due to favorable interactions between organic ligands and polymers.[55] Ge et al. synthesized ZIF-8 thin layer on an asymmetrically porous polyethersulfone (PES) substrate via secondary growth. The continuous ZIF-8 layer containing microcavities had good affinity with the PES support. Molecular sieving separation was achieved for selectively separating hydrogen from larger gases. At 333 K, the H_2 permeance could reach ~4×10^{-7} mol m^{-2} s^{-1} pa^{-1}, and the ideal selectivity of H_2 from Ar, O_2, N_2, and CH_4, were 9.7, 10.8, 9.9, and 10.7, respectively. The membrane showed stable hydrogen permeance and H_2/N_2 separation performance in the gas permeation tests. The binary gas selectivity exceeded the corresponding Knudsen selectivity.[56] In order to improve the performance of ZIF membrane supported on polymer substrate, the flexibility of polymer substrate should be reduced to avoid ZIF layer cracking.[57] Dehydrogenation, cyclization and crosslinking reaction of polyacrylonitrile (PAN) hollow fiber in solvothermal treatment could greatly improve the stiffness and compression strength of the support. A continuous and well intergrowth ZIF-8 membrane on PAN was successfully fabricated.[57] Nagaraju et al. prepared ZIF-8 membrane supported on a polysulfone based porous asymmetric ultrafiltration membrane by the Layer-by-Layer deposition of crystals and subsequent crystal growth. The H_2/C_3H_6 and H_2/CO_2 selectivity was increased by ~45% and 25%, respectively.[58]

ZIF-90 could be prepared through solvothermal reaction of zinc(II) salt and imidazolate-2-carboxyaldehyde (ICA),[25] and showed permanent microporosity with a narrow size of the six-membered ring pores (~3.5 Å). ZIF-90 was used as an example to show that it was possible to synthesize continuous ZIF membranes on polymeric hollow fiber surfaces by a facile, low-temperature, technologically scalable method. By dip-coating of ZIF-90 crystals (~400 nm) and secondary growth, continuous ZIF-90 membranes were fabricated on macroporous Torlon® (a polyamide-imide) hollow fibers.[59] Torlon was chosen as a suitable substrate polymer for separation applications because it is chemically resistant, withstands high pressures (up to 2000 psi) without plasticization, and is amenable to the engineering of hollow fibers of controlled macroporosity.[60] Single-gas permeation showed a strong trend of decreasing permeance with increasing kinetic diameter, showing that the permeation properties are mainly influenced by transport through the ZIF-90 pores and not through defects such as pinholes, cracks, or grain boundaries. The CO_2/N_2 and CO_2/CH_4 selectivities of 3.5 and 1.5, respectively are above the Knudsen selectivities (0.8 and 0.6), further confirming that gas transport is mainly through the ZIF-90 crystals. For the single-component pervaporation test, the permeance of n-hexane, benzene, and cyclohexane were 3900, 370 and 160 GPU (1 GPU $=1\times10^{-6}$ cm s^{-1} $cmHg^{-1}$).[59]

ZIFs have been used to improve the separation properties of other membranes. For example, vertically-aligned carbon nanotube forests fabricated by chemical vapor deposition (CVD) growth were made into membranes by filling epoxy into the interstices, followed by mechanical polishing to open the CNTs. These membranes had characteristically high permeation fluxes (1-2 orders greater than the Knudsen flow) and low hydrogen selectivities (H_2/Ar=4.14, H_2/O_2=3.82, H_2/N_2=3.48, H_2/CH_4=2.58 and H_2/CO_2=4.89).[61] To improve the gas separation performance, a ZIF-8 layer of about 5-6 μm was synthesized onto the surfaces of the aligned carbon nanotube membranes via secondary seeded growth. The ideal selectivities of H_2 to CO_2, Ar, O_2, N_2 and CH_4 of the ZIF-8 membrane were significantly improved, reaching up to 4.9, 7.0, 13.6, 15.1 and 9.8, respectively with a H_2 permeance of ca. 8.1×10^{-8} mol m^{-2} s^{-1} pa^{-1}.[61] Dumée reported the synthesis of the continuous, inter-grown ZIF-8 membrane via the secondary growth method on a carbon nanotube bucky-paper. ZIF-8 crystals were seeded and strongly anchored onto porous carbon nanotube bucky-paper supports and hydrothermally grown into a dense and continuous ZIF-8 network.[62] The high selectivity of N_2 over Xe demonstrated that the membranes were nearly defect-free and that the growth procedure was successful for creating an even interface between the CNTs and the ZIF-8 crystals. The low CO_2 selectivity over N_2 was shown to be related to very strong physisorption between the CO_2 and 2-methylimidazole molecules remaining within the ZIF-8 matrix. Mixed gas permeation tests (equimolar N_2/CO_2) confirmed this trend as nitrogen was found to permeate nearly 7 times faster than CO_2. The commercial anodic aluminum oxide (AAO) membrane was also used as the support to the preparation of ZIF-8/AAO composite membrane by a fast in situ seeding and secondary growth method.[63] ZIF-8 nanocrystals were plugged in the AAO nanochannels to form the separation layer and the ZIF-8/AAO composite membrane exhibited high gas separation performance with H_2/CO_2 and H_2/N_2 ideal selectivities of 6.38 and 4.19, respectively.

From the literature, it is clear that seeded secondary growth has been used as a predominant method for growth of ZIFs on different substrates. This method offers better controllability in the formation of membranes by tailoring the crystal size of ZIF seeds, the seeding density and the interactions between seeds and substrate and optimizing the secondary growth process.

Table 2. Single gas permeances and ideal selectivities of ZIF membranes discussed in the review.

Type	Substrate	Solvent	Membrane thickness (μm)	Synthesis method	Temp. (°C)	Permeance ($\times10^{-7}$ mol m^{-2} s^{-1} pa^{-1}) H_2	N_2	CO_2	CH_4	Ideal selectivity H_2/N_2	H_2/CO_2	CO_2/CH_4	Ref.
ZIF-8	titania	methanol	30	Direct synthesis	25	0.6	0.052	0.133	0.048	11.5	4.5	2.8	29
ZIF-8	alumina	methanol	25	Direct synthesis	25	2.4	0.20	0.46	0.18	12.0	5.2	2.56	33
SIM-1	alumina tube	DMF	25	Direct synthesis	30	0.82	0.33	0.36	-	2.5	2.27	-	27
ZIF-69	alumina	DMF	50	Direct synthesis	25	0.65	-	0.25	0.15	-	2.6	1.67	34
ZIF-8	alumina	water	2.5	Secondary growth	~23	3.6	0.9	1.3	0.8	4.0	2.8	1.6	39
ZIF-8	alumina hollow fiber	water	1.4	Secondary growth	25	75	19	-	-	3.9	-	-	42
ZIF-8	alumina hollow fiber	methanol	6	Repeated growth	25	5.2	2.1	0.16	1.9	2.5	32.2	0.08	43
ZIF-8	alumina tube	methanol	5	Secondary growth	25	11	1.51	2.12	1.62	7.3	5.2	1.31	44
ZIF-8	YSZ hollow fiber	water	2	Secondary growth	25	15.4	1.4	4.0	1.2	11.0	3.9	3.3	45
ZIF-7	alumina	DMF	1.5	Secondary growth	200	0.74	0.11	0.11	0.118	6.73	6.70	0.93	46
ZIF-7	alumina	DMF	2	Secondary growth	220	0.455	0.022	0.035	0.031	20.7	13.0	1.13	48
ZIF-69	alumina	DMF	40	Secondary growth	25		0.106	0.236	0.086			2.7	51
ZIF-8	alumina	methanol	~1	Layer-by-layer	35	0.19	0.019	0.041	0.02	11	5	2.05	52
ZIF-8	polyethersulfone	methanol	7.2	Secondary growth	60	4	0.04	-	-	9.9	-	-	56
ZIF-8	polyethersulfone	methanol	10	Layer-by-layer	25	1592 GPU	-	417 GPU	-	-	3.8	-	58
ZIF-90	Torlon®	methanol	5	Secondary growth	35	580 GPU	100 GPU	300 GPU	200 GPU	5.8	1.93	1.5	59
ZIF-8	carbon nanotube	methanol	5-6	Secondary growth	25	0.81	0.053	0.165	0.083	15.1	4.9	1.99	61

This journal is © The Royal Society of Chemistry [year]

ZIF-8	AAO membrane	methanol	-	Fast in situ seeding and secondary growth	25	1.34	0.32	0.21	-	4.19	6.38	-	63
ZIF-22	titania	DMF	40	APTES and secondary growth	50	2	0.28	0.24	0.299	7.1	8.5	0.80	64
ZIF-90	alumina	DMF	20	APTES and secondary growth	200	2.5	0.198	0.348	0.157	12.6	7.2	2.22	65
ZIF-90	alumina	DMF	20	APTES and secondary growth	200	2.1	0.128	0.134	0.108	16.4	15.7	1.24	66
ZIF-90	alumina	DMF	20	APTES and secondary growth	225	3.08	-	0.41	0.19	-	7.51	2.15	67
ZIF-95	alumina	DMF	30	APTES and secondary growth	325	24.6	2.27	7.04	1.61	10.8	34.9	4.37	68
ZIF-9-67	alumina	DMF	30-35	Organosilane modification	25	140.5	38.1	15.8	51.7	3.68	8.90	0.31	28
ZIF-8	alumina hollow fiber	water	2	APTES and cycling precursor	25	4.3	0.35	1.22	0.32	12.28	3.54	3.79	69
ZIF-8	alumina	methanol	12	Hot support seeding	25	1.75	0.15	0.47	0.14	11.6	3.72	3.4	70
ZIF-8	alumina hollow fiber	methanol	20	Hot support seeding	25	7.3	0.79	1.35	0.68	9.2	5.4	1.99	71
ZIF-8	alumina	methanol	10	Precursor filtration	25	1.7	0.3	-	-	5.7	-	-	72
ZIF-78	ZnO	DMF	25	Reactive seeding	25	1.02	0.15	0.093	0.17	6.6	11.0	0.66	73
ZIF-8	alumina hollow fiber	methanol	8	Reactive seeding	25	2.08	0.20	0.51	0.20	10.3	4.08	2.55	74
ZIF-8	Nylon	methanol	16	Contra-diffusion	25	19.7	4.6	-	-	4.3	-	-	54
ZIF-8	Nylon	water	2.5	Contra-diffusion	25	11.3	2.5	-	-	4.6	-	-	75
ZIF-8	alumina tube	methanol	2	Counter-diffusion	25	573	37.2	33.7	-	15.4	17.0	-	76
ZIF-8	alumina hollow fiber	methanol	70	Counter-diffusion	25	0.91	0.091	-	-	10	-	-	77

DMF: N,N-dimethylfomamide, 1 GPU =1×10^{-6} cm s^{-1} $cmHg^{-1}$

2.3. Surface functionalization and special seeding

Due to semi-organic nature of ZIFs, organic functionalization of substrate surface, creation of seeding layer by chemical reactions on the substrate, and post-functionalization have attracted growing attention, and they provide additional means for facilitating ZIF crystallization on substrates and modifying ZIF membrane surface, thus improving the quality of ZIF membranes.

2.3.1. Surface functionalization by covalent linkers and post-functionalization

In order to provide active sites for nucleation and enhance the adhesion between ZIF membranes and supports, many methods have been developed to modify the surface of the supports. In addition, post-functionalization has been carried out to improve the selectivity of membranes. In this section, the surface functionalization and post-functionalization by attaching different functional groups will be discussed.

ZIF-90 is a good candidate for separating H_2 from other large molecules. By using 3-aminopropyltriethoxysilane (APTES) as a covalent linker, a continuous ZIF-90 membrane was prepared by Huang and co-workers.[65] A preparation scheme is shown in Fig. 6. In the first step, the ethoxy groups of the APTES react with surface hydroxyl groups of the Al_2O_3 support. In the second step, the amino groups react with the aldehyde groups of imidazolate-2-carboxyaldehyde via imines condensation, and then the nucleation and crystal growth of the ZIF-90 start at these fixed sites on the surface of the porous ceramic supports. The ideal selectivities of H_2 from CO_2, N_2, CH_4, and C_2H_4 were 7.2, 12.6, 15.9, and 63.3, respectively, suggesting that ZIF-90 membrane displayed molecular sieving performance with a high H_2 permselectivity. For the 1:1 binary mixtures, the mixture separation factors of H_2/CO_2, H_2/N_2, H_2/CH_4, and H_2/C_2H_4 were 7.3, 11.7, 15.3, and 62.8, respectively, which by far exceeded the corresponding Knudsen selectivities (4.7, 3.7, 2.8, and 3.7, respectively).

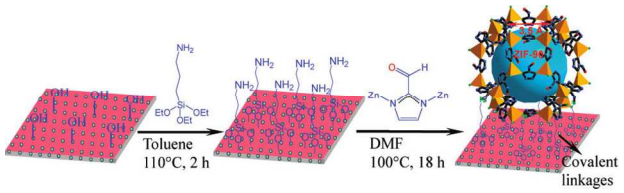

Fig. 6. Scheme of preparation of ZIF-90 membranes by using APTES as a covalent linker between ZIF-90 membrane and Al_2O_3 support via an imine condensation reaction. Reprinted with permission from ref. 65. Copyright 2010 American Chemical Society.

As reported by Yaghi and co-workers, the free aldehyde groups in the ZIF-90 framework allow the covalent functionalization with amine groups by an imine condensation reaction.[25] The covalent post-functionalization of a ZIF-90 membrane by ethanolamine to enhance its H_2/CO_2 selectivity was conducted by the same research group.[66] Two effects could be expected: the imine functionalization could constrict the pore aperture of ZIF-90 and prevents larger molecules from accessing the pores, and the covalent post-functionalization could reduce non-selective transport through invisible intercrystalline defects, thus enhancing the separation selectivity (Fig. 7). By covalent post-

functionalization, the H_2/CO_2 selectivity could be increased from 7.3 initially to 62.5. The modified ZIF-90 membrane showed good stability in 3 vol % steam at 200 °C for 48 h, and was stable at 325 °C in the H_2/CO_2 separation for at least 24 h.[66] Similarly, they used APTES to post-modify ZIF-90 by forming covalent linkages between the free aldehyde groups of the ZIF-90 and the amino group of APTES.[67] The post-functionalization process could be finished in 30 min by refluxing the ZIF-90 membrane in APTES methanol solution. However, the similar process using ethanolamine as reactant was rather long (usually over 10 h), leading to some decomposition of ZIF-90 material. [66,67,78] For equimolar binary mixtures at 225 °C and 1 bar, the separation factors of CO_2/CH_4, H_2/CO_2, H_2/CH_4, H_2/C_2H_6, and H_2/C_3H_8 mixtures were found to be 4,7, 20, 71, 250, and 458, and a relatively high H_2 permeance of about 2.9×10^{-7} mol m^{-2} s^{-1} pa^{-1} could be obtained to avoid pore blocking.[67,78]

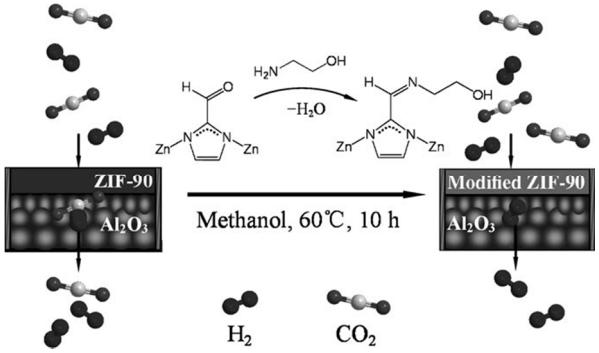

Fig. 7. Covalent post-functionalization of a ZIF-90 molecular sieve membrane by imine condensation with ethanolamine to enhance H_2/CO_2 selectivity. Reprinted with permission from ref. 66. Copyright 2011 John Wiley & Sons, Inc.

LTA topological ZIFs (ZIF-20, ZIF-21, and ZIF-22) were designed and synthesized by Yaghi and co-workers with high stability and high porosity.[13] ZIF-22 has the same pore size as ZIF-7 (about 0.3 nm), so ZIF-22 membranes are expected to display good molecular-sieving property for separation of H_2 from CO_2 and other larger gas molecules. Huang et al. used a seeding-free route to prepare ZIF molecular sieve membranes on porous ceramic supports by using APTES as covalent linker to promote nucleation and growth of ZIF-22.[64] The influence of surface chemistry of the substrate was improved after using APTES. On the contrary, separate ZIF-22 crystals and crystal islands rather than a continuous layer formed if the support surface was not treated with APTES before ZIF-22 crystallization. For ZIF-22 membrane at 323 K, the mixture separation factors of H_2/CO_2, H_2/O_2, H_2/N_2, and H_2/CH_4 are 7.2, 6.4, 6.4, and 5.2, respectively, with H_2 permeances higher than 1.6×10^{-7} mol m^{-2} s^{-1} pa^{-1}. POZ topology ZIF-95 shows a permanent microporosity with constricted windows (~0.37 nm) and huge cavities (2.4 nm), and could be prepared through solvothermal reaction of zinc (II) salt and 5-chlorobenzimidazole (cbIM).[26] ZIF-95 was fabricated on an APTES-modified porous alumina support and exhibited high selectivity for gas separation. The single gas permeances through the ZIF-95 membrane followed the order: $H_2>N_2>CH_4>CO_2>C_3H_8$, which mainly corresponded to their kinetic diameters with the exception of CO_2; H_2 permeance (2.46×10^{-6} mol m^{-2} s^{-1} pa^{-1}) was the highest due to its small kinetic diameter of 0.29 nm. For binary mixtures at 325 °C and 1 bar, the mixture separation factors of H_2/CO_2, H_2/N_2, H_2/CH_4 and H_2/C_3H_8 were 25.7, 10.2, 11.0 and 59.7, respectively. Furthermore, the ZIF-95 membrane showed a high thermal stability up to at least 325 °C and a hydrothermal stability in steam, thus offering a potential application in hydrogen production.[68] A hybrid ZIF-9-67 membrane on α-Al_2O_3 support was developed by using a mixed-linker synthesis method.[28] The alumina supported was modified with vinyltrimethoxysilane and then oxidized to terminating vinyl group. Compared with the existing ZIF membranes, this ZIF-9-67 hybrid membrane exhibited good ideal selectivities for H_2/CO_2, CH_4/CO_2, CO/CO_2, and N_2/CO_2 while having high permeances of H_2, CH_4, CO and N_2. Furthermore, the ZIF-9-67 hybrid membrane was less permeable to CO_2 than all other gases tested. Therefore, this membrane is very promising for efficient CO_2 removal from industrial mixtures that are composed of these gases.[28] As mentioned before, the addition of polyethyleneimine in the dip-coating solution was important to prepare continuous and dense membranes because the polyethyleneimine acted as the linkers between ZIF nanocrystals and the substrates.[36,46,48,50]

By using the organosilane as the binder, ZIF-8 films with controllable thickness were grown on a modified substrate at room temperature. The 3-(2-imidazolin-1-yl)propyltriethoxysilane (IPTES) was used to first form a pseudo-surface of ZIF-8 on a glass substrate, followed by layer-by-layer growth (Fig. 8). The film thickness of ZIF-8 was controlled within the range from 220 to 640 nm per growth cycle by changing the reactivity of the zinc source. The reactivity of zinc acetate was lower than that of zinc nitrate at the same concentration, and dense ZIF-8 films were obtained using a low reactivity growth solution.[79] By the similar technique, (110)-oriented ZIF-8 thin films with controllable thickness were deposited on indium tin oxide (ITO) electrodes at room temperature. APTES was used as the covalent linkers, and the layer-by-layer method was then applied to coat the ZIF-8 thin films. The observed cross-sectional SEM images and fluorescence spectra of the ZIF-8 thin films indicated that the number of layers grown was proportional to the number of immersion cycles. The crystallographic preferential orientation (CPO) index showed that the ZIF-8 thin films were (110)-oriented. [80]

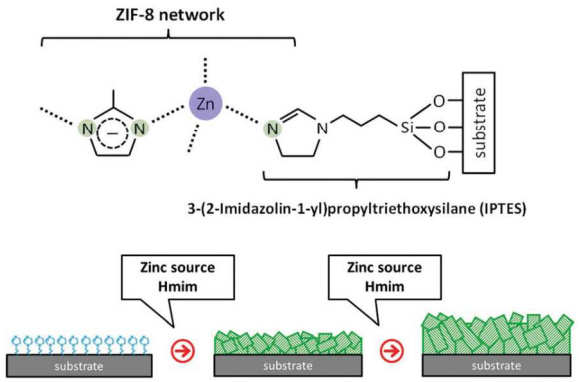

Fig. 8. Strategy for the preparation of the ZIF-8 films by using organosilane as binder. Reproduced from Ref. 79.

A ZIF-8 membrane was successfully grown on inner surface of

This journal is © The Royal Society of Chemistry [year]

hollow fiber from cycling precursors (Fig. 9). APTES effectively enhanced the heterogeneous nucleation of the ZIF-8 crystals. After the modified in-situ seeding process, a strong adhesive and uniform ZIF-8 seeding layer was formed on the inner surface of the APTES modified ceramic hollow fiber in a single step. The as-prepared inner-side hollow fiber ZIF-8 membrane was of high integrity and thin. The ideal selectivities of H_2 over CO_2, N_2, and CH_4, are 3.54, 12.28 and 13.41, respectively. The permeation behaviors of binary gas mixtures (H_2/CO_2, H_2/N_2 and H_2/CH_4 with an equal volume ratio) were also studied. As the separation factors of H_2/CO_2, H_2/N_2 and H_2/CH_4 were 3.28, 11.06 and 12.13, respectively.[69]

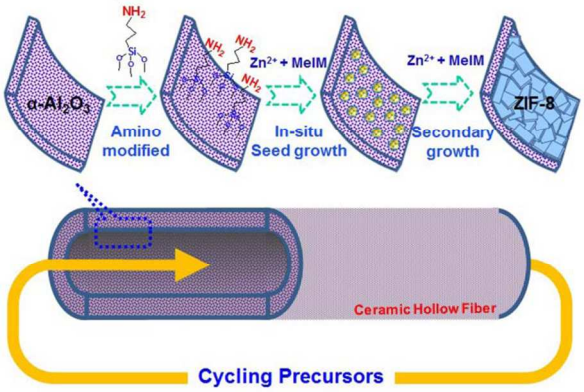

Fig. 9. Schematic diagram of growth of the inner-side hollow fiber ZIF-8 membrane. Reproduced from Ref. 69.

2.3.2. Surface special seeding

In addition to the formation of functional linkers on substrate surface, a number of other methods including imidazolate deposition, precursor infiltration and reactive seeding, have been shown to be effective for substrate modification for facilitating ZIF crystallization. Jeong et al. reported the hot support modification by imidazolate linkers (Fig. 10) to create strong covalent bonds between α-Al_2O_3 supports and imidazolate ligands, which promoted the heterogeneous nucleation and growth of ZIF crystals. ZIF-8 membrane was then prepared by the solvothermal synthesis, and the resulting ZIF-8 membranes was continuous and well-intergrown with a thickness of ca. 12 μm, exhibiting ideal selectivities of 11.6 and 13 for H_2/N_2 and H_2/CH_4, respectively.[70] ZIF-7 films were also fabricated to demonstrate the potential for general applicability of this method. Tao et al. used the hot dip-coating seeding method to prepare alumina hollow fiber supported ZIF-8 membrane.[71] A preheated alumina hollow fiber (150 °C, 4 h) was immediately dipped into a 1.5 wt% ZIF-8 seed suspension for 20 seconds. The dispersed ZIF-8 crystals rapidly moved to the support and sank into the support channels under the capillary and vacuum forces during this process. Thus, a uniform and robust seed layer could be formed on the support. Subsequently, the seeded support was dried and subjected to a solvothermal synthesis. The resulting ZIF-8 membrane revealed a molecular sieving behavior, and the ideal selectivities for H_2/CO_2, H_2/O_2, H_2/N_2 and H_2/CH_4 were calculated to be 5.4, 7.1, 9.2 and 10.8, respectively, which are much higher than corresponding Knudsen factors.[71]

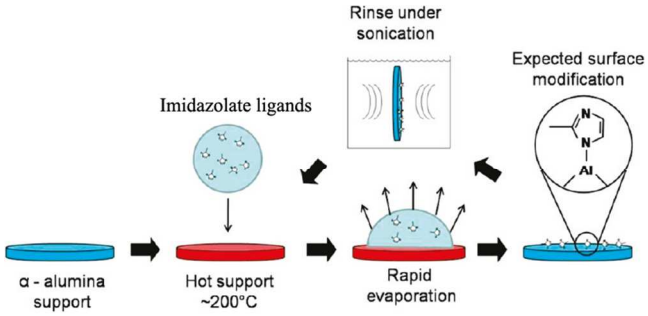

Fig. 10. Illustration of the substrate modification process. Reprinted with permission from ref. 70. Copyright 2010 American Chemical Society.

By infiltrating precursors into a porous alumina support as a seed-and-nutrient layer, Li et al. developed a new method to synthesize ZIF-8 membrane.[72] The alumina support was immersed in melting 2-methylimidazole (~145 °C) and then hydrothermally treated at zinc nitrate aqueous solution. A precursor layer with a thickness of about 10 μm was formed inside the porous alumina support, and after solvothermal synthesis, the ZIF-8 membrane grew from both the seeds embedded in the precursor layer and the synthesis solution under solvothermal synthesis conditions. A continuous and stable ZIF-8 membrane with a thickness of ca. 12 μm and an intermediate layer of ca. 10 μm was prepared at 120 °C for 8 h (Fig. 11). Gas permeation tests indicated the membrane was continuous and compact, and had H_2/N_2 ideal selectivity of 5.7 with a H_2 permeance of 1.7×10^{-7} mol m^{-2} s^{-1} Pa^{-1}.[72] An electrospinning technique has also been introduced into the synthesis of supported microporous membranes. A continuous and uniform seed coating composed of ZIF-8 and polyvinylpyrrolidone (PVP) was coated on the support surface, and the thickness of the seed layer could be precisely controlled. ZIF-8 membrane was then prepared by the secondary growth method. The resulting ZIF-8 membranes exhibited H_2/N_2, H_2/CO_2 and H_2/CH_4 separation factor of 4.94, 7.31, and 4.84, respectively, with the H_2 permeance of about 3.3×10^{-7} mol m^{-2} s^{-1} pa^{-1}.[81] By electrospinning of ZIF-8 and PVP mix solution, it was possible to fabricate the self-supported non-woven ZIF-8/PVP fiber mat. The adsorption measurements showed that the ZIF-8 nanoparticles were fully accessible, and such ZIF textile could be useful for gas adsorption and separation.[82]

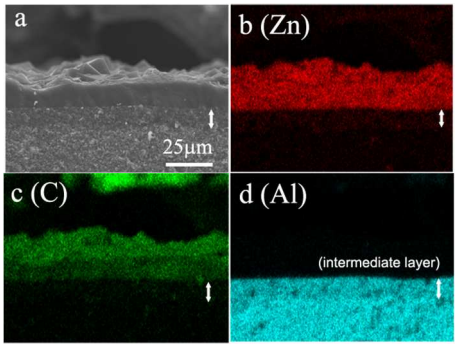

Fig. 11. SEM image (a) of the cross-section of ZIF-8 membrane prepared at 120 °C for 8 h and its EDX elemental mapping images: Zn (b), C (c) and Al (d). Reprinted with permission from ref. 72. Copyright 2013 Elsevier.

The reactive seeding method was first developed for the preparation of continuous MOF MIL-53 and MIL-96 membranes on alumina porous supports, in which the porous support acted as the inorganic source reacting with the organic precursor to grow a seeding layer.[83] Dong et al. used the reactive seeding method to prepare ZIF-78 membrane on ZnO support.[73] The GME ZIF-78 consists of divalent zinc cations bridging by 2-nitroimidazolate and 5-nitrobenzimidazolate anions, and the cage size in ZIF-78 is 7.1 Å and the window size is 3.8 Å. However, the removal of organic solvents from the ZIF crystals is one of the key steps and a challenge in preparing high-quality ZIF membranes. For instance, given that DMF has a kinetic diameter of 5.5Å, it is not easy to remove it through the narrower ZIF-78 windows due to the relatively rigid imidazolate frameworks, and hence DMF removal may induce intercrystalline defects or even cracks in the membranes and a loss of performance. The authors used a new solvent activation-exchange method to achieve effective removal of DMF, where a series of methanol-DMF mixtures with different methanol concentrations of 25, 50, 75 and 100 vol% were used. The membrane activation process is illustrated in Fig. 12.[73] The single gas permeation of H_2, N_2, CH_4, and CO_2 was tested on ZIF-78 membrane, and the permeance of these small gas molecules decreases in the order H_2 >N_2 >CH_4 >CO_2, with increasing the molecular sizes except for CO_2. The ideal selectivities of H_2/CO_2, H_2/N_2 and H_2/CH_4 are 11.0, 6.6 and 6.0, respectively.[73] The relatively low permeance of CO_2 was attributed to the strong interaction between CO_2 and ZIF-78 frameworks because of the dipole-quadrupole interactions between -NO_2 and CO_2.[24] For the binary gas mixture, the separation factors of H_2/CO_2, H_2/N_2 and H_2/CH_4 were 9.5, 5.7 and 6.4, respectively. All these mixture-separation factors exceeded the corresponding Knudsen diffusion selectivity values.[73] ZIF-8 was also grown on alumina hollow fibers by the reactive seeding method.[74] A 0.5 μm thick nanoporous ZnO layer was deposited on the inner surface of the hollow fiber by the slip-casting method. The hollow fiber was then treated with 2-methylimidazole solution to activate the ZnO layer for ZIF-8 deposition, followed by the secondary growth to prepare the low-defect ZIF-8 layer with a thickness of about 8 μm. The ZIF-8 membrane showed a high H_2 permeance of 2.08×10^{-7} mol m^{-2} s^{-1} pa^{-1} with H_2/N_2, H_2/CH_4, H_2/C_3H_8, H_2/n-C_4H_{10} and H_2/SF_6 ideal selectivities of 10.3, 10.4, 149.6, 195.7 and 281.5, respectively.[74] Table 3 summarizes the mixed gas separation data obtained from various ZIF membranes discussed in this review for easy comparison (more details in S-Table 1, Supplementary Information).

Despite the gas separation has been the main focus for the development of ZIF membranes, liquid separation via pervaporation using ZIF membranes has also been demonstrated. By the same reactive seeding method, an integrated ZIF-71 membrane was prepared for the first time and used for pervaporation separation of alcohol (methanol and ethanol)-water and dimethyl carbonate (DMC)-methanol mixtures. The ZnO support was used to react with 4,5-dichloroimidazole (dcIm) to produce the seed layer. The ZIF-71 membrane showed good pervaporation performance especially in DMC-methanol separation. The total flux and separation factor in the separation of 5 wt% DMC-MeOH at 25 °C were 271 g m^{-2} $h^{-1}$and 5.34, respectively.[84] Fan et al. developed a novel approach to synthesize ZIF-78 membrane by replacing the crystal seeds with nanosized amorphous ZIF-78 precursors, which could provide better distributed nucleation sites.[85] During the secondary growth process, the crystal size and intergrowth degree of the membrane was adjusted by adding triethylamine to the reaction solution. The high quality membrane synthesized under this method was tested for pervaporation separation of cyclohexanone/cyclohexanol mixture with equal volume ratios at room temperature with permselectivity of 1:2 and total flux around 8.7×10^{-2} kg m^{-2} h^{-1}.[85] The above work demonstrated that ZIF-71 and ZIF-78 were promising membrane materials for the pervaporation separation of not only organics-water but also organics-organics systems.

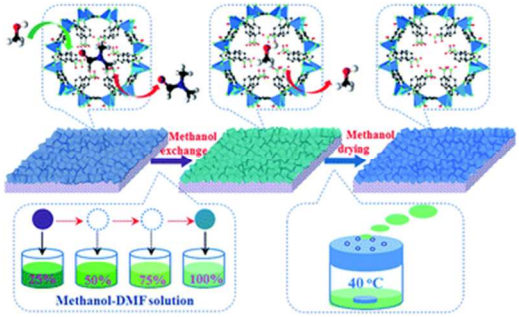

Fig. 12. Schematic diagram of the activation process of the ZIF-78 membrane. Reproduced from Ref.73.

The stability of ZIF materials and membranes is crucially important for the practical applications. ZIF materials show high thermal stability and remarkable chemical resistance to boiling solvents, such as methanol, benzene and water.[1,2] Recent studies suggest that ZIF membranes are quite stable in gas phases. For example, a month-long stability test showed stable gas permeance and separation performance of the ZIF-8 membranes in both atmospheric condition and C_3H_6/C_3H_8 mixture stream.[41] However, the stability of ZIF membranes in organic solvents has not been extensively studied. The stability of ZIF-78 membrane for pervaporation separation of equimolar cyclohexanone/cyclohexanol mixture was tested for 50 h. The total flux had a distinct decrease in the initial 16 h, and then became stable throughout the remaining test, indicating some changes in the ZIF-78 membrane. No further details were reported.[85] Recently, the stability of MOF-5 membrane during pervaporation of organic solvents was examined. The on-stream xylene permeation flux of as-synthesized MOF-5 membrane decreased and reached a steady-state value about 70% of the initial flux value after 16 h on stream. There was no microstructural degradation occurred, but showed evidence of retained xylene isomers (fouling) in the MOF-5 structure.[86] Despite the fact that MOF-5 has different crystal topology, this study may provide valuable insights into the solvent stability of ZIF membranes. It is worth noting that pervaporation through ZIF membranes sometimes give interesting and unpredictable results.[84,86,87] ZIF-71 showed good permselectivity for DMC over methanol despite DMC having a larger kinetic diameter than methanol due to the weaker polarity of the DMC molecules.[84] More studies are clearly required to elucidate the solvent stability and structural change mechanism of ZIF membrane in organic solvents.

This journal is © The Royal Society of Chemistry [year]

Cite this: DOI: 10.1039/c0xx00000x

www.rsc.org/xxxxxx

ARTICLE TYPE

Table 3. Mixed binary gas (1:1) separation data obtained from various ZIF membranes discussed in this review.

Type	Substrate	Solvent	Membrane thickness (μm)	Synthesis method	Temp. (°C)	Separation factor					Ref.
						H_2/N_2	H_2/CO_2	H_2/CH_4	C_3H_6/C_3H_8	CO_2/CH_4	
ZIF-8	titania	methanol	30	Direct synthesis	25	-	-	11.2	-	-	29
ZIF-8	tubular alumina	methanol	5-9	Secondary growth	22	-	-	-	-	4.1-7.0	35
ZIF-8	alumina	methanol	12	Secondary growth	25	-	6.5	17	-	-	36
ZIF-8	alumina	water	2.2	Secondary growth	-15	-	-	-	~50	-	40
ZIF-8	alumina	water	2.5	Secondary growth	35	-	-	-	30	-	41
ZIF-8	alumina hollow fiber	methanol	6	Repeated growth	25	-	7.1 (45% H_2)	-	-	-	43
ZIF-7	alumina	DMF	1.5	Secondary growth	200	7.74	6.48	5.92	-		46
ZIF-7	alumina	DMF	2	Secondary growth	220	18	13.6	14	-		48
ZIF-7	alumina	DMF	2	Microwave assisted secondary growth	200	-	8.4	-	-	-	50
ZIF-69	alumina	DMF	40	Secondary growth	25	-	-	-	-	4.6	51
ZIF-22	titania	DMF	40	APTES and secondary growth	50	6.4	7.2	5.2	-	-	64
ZIF-90	alumina	DMF	20	APTES and secondary growth	200	11.7	7.3	15.3	-	-	65
ZIF-90	alumina	DMF	20	APTES and secondary growth	200	15.8	15.3	18.9	-	-	66
ZIF-90	alumina	DMF	20	APTES and secondary growth	225	-	21.6	79.6	-	-	67
ZIF-90	alumina	DMF	20	APTES and secondary growth	225	-	-	-	-	4.7	78
ZIF-95	alumina	DMF	30	APTES and secondary growth	325	10.1	25.7	11.0	-	-	68
ZIF-8	alumina hollow fiber	water	2	APTES and cycling precursor	25	11.06	3.28	12.13	-	-	69
ZIF-78	ZnO	DMF	25	Reactive seeding	25	5.7	9.5	6.4			73
ZIF-8	polyvinylpyrrolidone	DMF	80	Electrospinning and secondary growth	25	4.94	7.31	4.84	-	-	81
ZIF-8	alumina	methanol	1.5	Counter-diffusion	20	-	-	-	55	-	88
ZIF-8	alumina	water	1.5	Counter-diffusion	20	-	-	-	40.43±8.45	-	89
						H_2/C_3H_8	H_2/C_3H_6	C_2H_6/C_3H_8	C_2H_4/C_3H_6	C_2H_4/C_3H_8	
ZIF-8	alumina	methanol	12	Secondary growth	25	~390	-	-	-	-	36
ZIF-8	alumina	water	2	Secondary growth	23	545	23	80	10	167	39

2.4. Contra-diffusion (counter-diffusion) synthesis

In the contra-diffusion synthesis, two precursor solutions (e.g., metal ion solution and organic ligand solution) separated by a porous substrate counter-diffuse through the porous channels of the substrate; ZIF nucleation and crystallization start on the substrate when the two solutions meet with each other. Such a methodology is similar to that developed for mesoporous silica and zeolite membrane synthesis.[90-92] But in the ZIF synthesis, diffusion rates of metal ion solution and imidazolate solution can be different because of their different interactions with the substrates. Therefore, in conjunction with surface modification and seeding of substrate, the contra-diffusion method provides more degrees of freedom in controlling the synthesis of ZIF membranes.

Yao et al. for the first time extended the contra-diffusion method to prepare ZIF-8 on a macroporous Nylon membrane. [54] Zinc nitrate methanol solution and 2-methylimidazole methanol solution are separated by the porous Nylon membrane (Fig. 13a). Similar to the synthesis of single crystals by slow diffusion,[22] the

two solutions crossover the Nylon membrane and crystallize at the interface (Fig. 13b). After 72 h of contra-diffusion synthesis, a continuous film with a thickness of ca. 16 μm was formed on the zinc side, and exhibited a H_2/N_2 ideal selectivity of 4.3 with H_2 permeance of 1.97×10^{-6} mol m^{-2} s^{-1} Pa^{-1} and N_2 permeance of 0.46×10^{-6} mol m^{-2} s^{-1} Pa^{-1}. By using the same contra-diffusion method, ZIF-8 films were prepared on both sides of Nylon membrane in aqueous solutions using a stoichiometric ratio of Zn^{2+} and 2-methylimidazole (hmim) with the addition of ammonium hydroxide.[75] ZIF-8 films prepared with a Zn^{2+}: hmim: NH_4^+ molar ratio of 1: 2: 32 at room temperature for 24 h exhibited an intergrown ZIF-8 layer on hmim side with a thickness of ca. 2.5 μm, which was greatly reduced compared to that prepared in methanol solvent. The membrane exhibited H_2 and N_2 permeation of 1.13×10^{-6} and 2.45×10^{-7} mol m^{-2} s^{-1} pa^{-1}, respectively, with a H_2/N_2 ideal selectivity of 4.6.

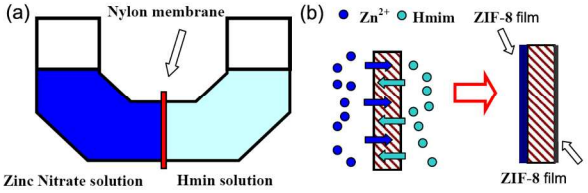

Fig. 13. (a) Diffusion cell for ZIF-8 film preparation and (b) the schematic formation of ZIF-8 films on both sides of nylon support via contra-diffusion of Zn^{2+} and Hmim through the pores of Nylon support. Reproduced from Ref.54.

Yang et al. further modified the contra-diffusion method to promote ZIF-8 growth on substrate. They chemically modified the support by depositing 3-aminopropyltriethoxysilane (APTES)-functionalized Al_2O_3 particles onto a coarse macroporous support (Fig. 14). The two synthesis solutions: zinc nitrate solution and 2-methylimidazole solution were separated by the deposited support, and the crystallization was carried out at 150 °C for 5 h. APTES grafted on the α-Al_2O_3 particles played an important role in growth of ZIF-8 membrane. A continuous, defect-free and thin ZIF-8 membrane was successfully prepared and exhibited remarkably high H_2 permeance of 5.73×10^{-5} mol m^{-2} s^{-1} pa^{-1} with H_2/N_2 and H_2/CO_2 ideal selectivity of 15.4 and 17.0, respectively.[76] Very recently, Hara et al. prepared ZIF-8 membranes on the outer surface of porous alumina hollow fibers using the counter diffusion method, resulting in the formation of an 80 μm-thick ZIF-8 layer.[77] The zinc nitrate methanol solution was kept in the inner section of the hollow fiber, and then immersed the hollow fiber in the 2-methylimidzole methanol solution at 50 °C for a predefined reaction time (e.g. 72 h). The ZIF-8 membrane permeances of hydrogen and propylene reached 9.1×10^{-8} and 2.5×10^{-9} mol·m^{-2}·s^{-1}·Pa^{-1}, respectively. The ideal selectivities for H_2/C_3H_8 and C_3H_6/C_3H_8 at 25 °C were found to be 2000 and 59, respectively.[77]

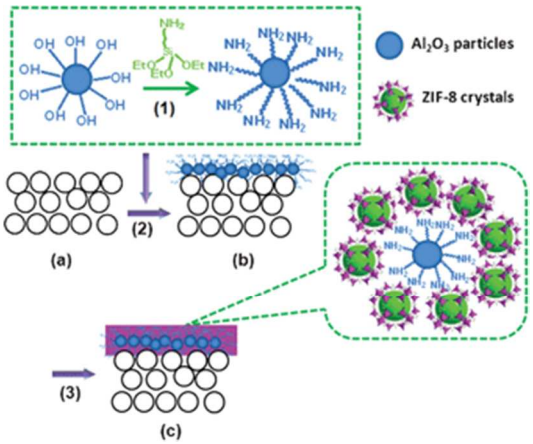

Fig. 14. Schematic diagram of the "two-in-one" strategy of deposition of chemically modified α-Al_2O_3 particles onto the support for preparation of ZIF-8 membrane: (a) support; (b) support with deposition of chemically modified α-Al_2O_3 particles; (c) ZIF-8 membrane constructed on the deposited support prepared using chemically modified α-Al_2O_3 particles. Reproduced from Ref.76.

Jeong et al. developed *in situ* counter-diffusion method to form ZIF-8 membranes. The zinc source was pre-deposited in the porous alumina support and then diffused out in the 2-methylimidazole solution to form ZIF-8 membrane at the interface of the porous support (Fig. 15) under solvothermal synthesis for 4 h at 120 °C, and the resulting ZIF-8 membranes exhibited high separation performance toward propylene over propane.[88] The high-quality ZIF-8 membranes showed an excellent separation performance for a propylene/propane (50/50) mixture (selectivity ~55). Furthermore, the ZIF-8 membranes were found to be mechanically very strong with their separation performance maintained high even after 2 h of intensive sonication. The prototypical ZIF-7 and SIM-1 membranes were also successfully synthesized using this counter-diffusion method. Similarly, by using microwave heating, a densely packed ZIF-8 seed layer could be rapidly formed on porous alumina supports in the aqueous solution by the same research group.[89] The microwave seeding process involves three steps: (1) saturation of a porous support with a metal precursor solution, (2) exposure of the support soaked with metal ions to a ligand precursor solution, and (3) rapid crystal formation under microwave irradiation. It is critically important to maintain relatively high concentrations of both metal ions and ligand molecules in the vicinity of the support ("reaction zone") by soaking the support with metal ions prior to microwave irradiation. The high-quality ZIF-8 membranes exhibited an average propylene/propane selectivity of ca. 40. The unique feature of the counter-diffusion synthesis allowed the poorly intergrown membranes to be healed. Furthermore, ZIF-7 and SIM-1 membranes were also synthesized using this method to demonstrate its potentially general applicability.

This journal is © The Royal Society of Chemistry [year]

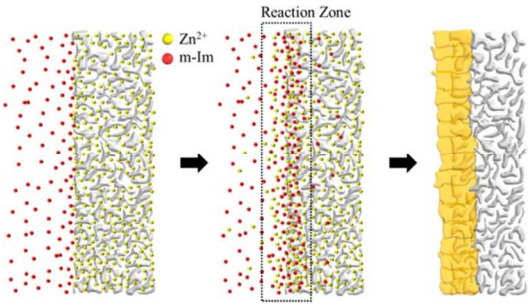

Fig. 15. Schematic illustration of the membrane synthesis using the counter-diffusion-based *in situ* method: (1) A porous alumina support saturated with a metal precursor solution is placed in a ligand solution containing sodium formate; (2) the diffusion of metal ions and ligand molecules cause the formation of a "reaction zone" at the interface; and (3) rapid heterogeneous nucleation/crystal growth in the vicinity at the interface leads to the continuous well-intergrown ZIF-8 membranes. Reprinted with permission from ref. 88. Copyright 2013 American Chemical Society.

3. ZIF/polymer mixed matrix membranes

Mixed matrix membranes are another important class of membranes being pursued over the last decades. They are composed of a polymer and a dispersed additive, and have great potential to achieve high separation properties and scale up for industrial applications by taking advantage of both materials. In a dense polymer membrane, the separation process is based on the solution-diffusion mechanism (Fig. 16). The selectivity is determined by two factors: the components solubility and the diffusivity.[93] Many studies have shown that the separation properties of polymer membranes can be significantly improved by incorporation of a dispersed phase including carbon molecular sieves, zeolites, mesoporous materials, activated carbons, carbon nanotubes, and metal-organic frameworks.[19,55,94-96] The composite membranes thus prepared are commonly referred to as mixed matrix membranes (MMMs).

The Maxwell model as shown below has been widely used for the performance prediction of mixed matrix membranes:[94]

$$P_{eff} = \mathrm{P_c}\left[\frac{\mathrm{P_D} + 2\mathrm{P_c} - 2\emptyset_\mathrm{D}(\mathrm{P_c} - \mathrm{P_D})}{\mathrm{P_D} + 2\mathrm{P_c} + \emptyset_\mathrm{D}(\mathrm{P_c} - \mathrm{P_D})}\right]$$

where P_{eff} is the effective permeability, P_C and P_D represent the permeabilities of the continuous phase and dispersed phase, respectively, and Φ_D is the volume fraction of the dispersed phase.

Like other mixed matrix membranes, ZIF/polymer membranes are usually prepared by dispersing ZIF particles in a polymer solution and using conventional polymer membrane fabrication techniques such as solution casting and hollow fiber spinning. However, in many cases, there exists a significant problem associated with the compatibility of the polymeric and inorganic phases for optimum dispersion and interfacial contact,[97,98] which only allows for moderate loadings of dispersed materials.

Compared with other materials, ZIFs (MOFs) with functional ligands intrinsically have better compatibility; importantly, many different types of ZIFs are available, ZIF/polymer mixed matrix membranes with more functionalities can be developed.

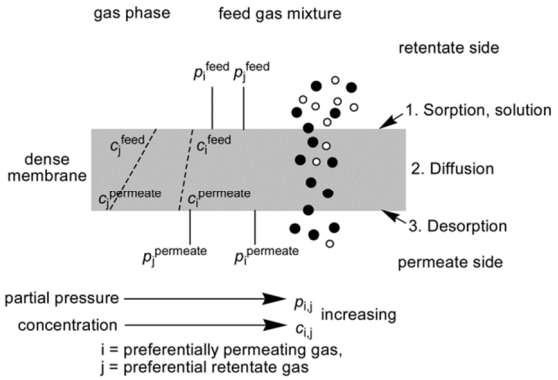

Fig. 16. Simplified and schematic separation mechanism in dense membranes by solution–diffusion. Reproduced from Ref.93.

3.1. Symmetrical dense composite membrane for gas separation

Polyimides are very attractive for gas separation due to their high gas selectivity, high chemical, thermal, and mechanical resistance. ZIF-8/Matrimid® MMMs were fabricated with loadings up to 80 wt%, which were much higher than the typical loadings achieved with selected zeolite materials. Only at the highest loading did the ZIF-8/Matrimid® composite membrans show a loss of mechanical strength, leading to a decrease in flexibility. The ZIF-8/Matrimid® MMMs permeation properties were tested for H_2,CO_2,O_2,N_2,CH_4, C_3H_8, and gas mixtures of H_2/CO_2 and CO_2/CH_4. The permeability values increased as the ZIF-8 loading increased to 40% (w/w). However, at higher loadings of 50% and 60% (w/w), the permeability decreased for all gases, and the selectivities increased consistent with the influence of the ZIF-8 additive. The ideal selectivities of gas pairs containing small gases, such as H_2/O_2, H_2/CO_2, H_2/CH_4, CO_2/CH_4, CO_2/C_3H_8, and H_2/C_3H_8, showed improvement with the 50% (w/w) ZIF-8 loading, demonstrating a transition from a polymer-dominated to a ZIF-8-controlled gas transport process.[99] Song et al. directly incorporated as-synthesised ZIF-8 nanoparticles (~60 nm) into a model polymer matrix (Matrimid® 5218) by solution mixing, and produced flexible transparent membranes with excellent dispersion of nanoparticles and good adhesion within the polymer matrix. Pure gas permeation tests showed enhanced permeability of the mixed matrix membrane with negligible losses in selectivity. For the ZIF-8/Matrimid membrane with a 20% ZIF-8 loading, the permeability of H_2, CO_2, O_2, N_2 and CH_4 was 63.53, 16.63, 5.63, 0.88 and 0.46 Barrer, respectively, with H_2/N_2, H_2/CH_4, CO_2/CH_4 and O_2/N_2 ideal selectivity of 72.5, 137.0, 35.8 and 6.4, respectively.[100] Table 4 summarizes the ZIF/polymer mixed matrix membranes and their performance for gas separation and pervaporation. In addition, for the ZIF-8/Matrimid® composite membranes, the ultrasonication treatment induced significant changes in the shape, size distribution, and structure of ZIF-8 particles suspended in an organic solvent during membrane processing. The membrane with 25 wt% ZIF-8 loading fabricated with high-intensity sonication showed significantly enhanced CO_2 permeability (23.2 Barrers) and increased CO_2/CH_4 ideal selectivity (39). In contrast, the composite membranes prepared with low-intensity sonication were found to be defective.[101] Positron annihilation lifetime spectroscopy (PALS) indicated that the increase in the free volume of the polymer with ZIF-8 loading

together with the free diffusion of gas through the cages of ZIF-8 contributed to an increase in gas permeability of the composite membrane, and the gas transport properties of the composite membranes could be well predicted by Maxwell model.[100]

Yang et al. demonstrated, for the first time, the incorporation of ZIF-7 nanoparticles into the polybenzimidazole (PBI) polymer matrix without much ZIF agglomeration by using an excessive amount of benzimidazole during the ZIF-7 synthesis. PBI was specifically chosen because it has remarkable resistance to high temperatures (up to 500 ^{o}C) with superior compression strength. In addition to exhibiting characteristics of high transparency and mechanical flexibility, the resultant composite membranes showed superior separation performance with enhanced H_2 permeability and ideal H_2/CO_2 permselectivity compared to both neat PBI and ZIF-7 membranes.[102] For the composite membranes, the gas permeability of H_2 exhibited significant enhancement with increasing ZIF-7 loadings, from 3.7 Barrer for pure PBI to 26.2 Barrer for 50/50 (w/w) ZIF-7/PBI, while the ideal selectivity of H_2/CO_2 improved from 8.7 to 14.9. For the H_2/CO_2 binary mixture, the separation factor of H_2/CO_2 was almost the same (6.8-7.2) with increasing ZIF-7 loading, but the H_2 permeability increased from 2.9 Barrer for pure PBI to 13.3 Barrer for 50/50 (w/w) ZIF-7 PBI.[102] In another attempt, ZIF-8 nanoparticles were incorporated into PBI, and the 30/70 ZIF-8/PBI dense membrane had a H_2 permeability of 105.4 Barrer and a H_2/CO_2 ideal selectivity of 12.3 at 180 ^{o}C.[103] This performance is far superior to ZIF-7/PBI membranes.[102] Intercalation may occur when the local particle loading is high enough that some of them bridge with one another across the entire membrane thickness. As a result, gas penetrants preferentially transport across the membranes via low-selectivity ZIF-8 particles (Fig. 17). The incorporation of ZIF-8 particles significantly enhanced both solubility and diffusion coefficients but the enhancement in diffusion coefficient was much greater. Mixed H_2/CO_2 separation tests were conducted from 35 to 230 ^{o}C, and ZIF/PBI membranes exhibited remarkably high H_2 permeability and H_2/CO_2 selectivity. The 30/70 (w/w) ZIF-8/PBI membrane had an H_2/CO_2 selectivity of 26.3 with an H_2 permeability of 470.5 Barrer, while the 60/40 (w/w) ZIF-8/PBI membrane had an H_2/CO_2 selectivity of 12.3 with an H_2 permeability of 2014.8 Barrer at 230 ^{o}C. However, at 35 ^{o}C, the 60/40 (w/w) ZIF-8/PBI membrane had an H_2/CO_2 slectivity of only 2.8 with an H_2 permeability of 669.9 Barrer. Mixed gas data showed that the presence of CO or water vapor impurity in the feed gas stream did not significantly influence the membrane performance at 230 ^{o}C.[104]

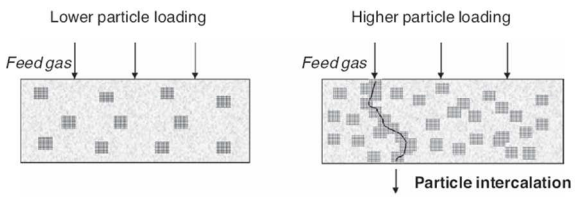

Fig. 17. Proposed scheme for gas transportation paths through the nanocomposite membranes at lower and higher particle loadings. Reprinted with permission from ref. 103. Copyright 2012 John Wiley & Sons, Inc.

It was observed that the solubility coefficient of CO_2 increased from 6.6×10^{-2} cm^3 (STP) cm^{-3} $cmHg^{-1}$ for the PPEES (poly(1,4-phenylene ether-ether-sulfone)) membrane to 0.116 cm^3 (STP) cm^{-3} $cmHg^{-1}$ for the membrane with 30% (w/w) of ZIF-8 filler.[105] Díaz et al. also fabricated ZIF-8/PPEES mixed matrix membrane.[106] The incorporation of ZIF-8 increased the permeability coefficient without significantly affecting the ideal selectivity. The higher the ZIF-8 loading the better the membranes permeability; and the diffusive process was mainly responsible for the selectivity of the membranes.[105,106] The ideal selectivity of the ZIF-8/PPEES membrane (ZIF-8 30 wt%) for O_2/N_2 and H_2/N_2 at 303 K was close to that marked by the Robeson upper-bound for this pair of gases, whereas that of H_2/CH_4 and CO_2/CH_4 was about 50% of that predicted in the Robeson limit. The ideal selectivity for C_2H_4/C_2H_6 was 3, with a C_2H_4 permeability of 3.15 Barrer.

Using three 6FDA-based polyimides (6FDA-Durene, 6FDA-Durene/DABA (9/1), 6FDA-Durene/DABA (7/3), Fig. 18) and nanosized ZIF-8, mixed matrix membranes with uniform morphology and as high as 40 wt% ZIF-8 loading were preparedy by directly mixing as-synthesized ZIF-8 suspension into the polymer solution.[107] Permeability of all gases (CO_2, CH_4, C_3H_6, and C_3H_8) increased rapidly with increasing ZIF-8 loading. However, the addition of ZIF-8 nanoparticles into the polymer matrix increased the CO_2/CH_4 ideal selectivity of only 6.87%, while the C_3H_6/C_3H_8 ideal selectivity improved by 134% from 11.68 to 27.38 for 6FDA-Durene/DABA (9/1) and 40 wt% ZIF-8. MMMs made of 6FDA-Durene did not show considerable improvements on resistance against CO_2-induced plasticization after annealing at 200-400 ^{o}C, while MMMs synthesized from cross-linkable co-polyimides (6FDA-Durene/DABA (9/1) and 6FDA-Durene/DABA (7/3)) showed significant enhancements in CO_2/CH_4 and C_3H_6/C_3H_8 selectivity as well as plasticization suppression characteristics up to a CO_2 pressure of 30 atm after annealing at 400 ^{o}C due to the cross-linking reaction of the carboxyl acid (COOH) in the DABA moiety. The MMM made of 6FDA-Durene/DABA (9/1) and 40 wt% ZIF-8 possessed a notable C_3H_6/C_3H_8 ideal selectivity of 27.38 and a remarkable C_3H_6 permeability of 47.3 Barrers. After being thermally annealed at 400 ^{o}C, the MMM made of 6FDA-Durene/DABA (9/1) and 20 wt% ZIF-8 showed a CO_2/CH_4 selectivity of 19.61 and an impressive CO_2 permeability of 728 Barrer in mixed gas tests.[107] ZIF-8 nanoparticles were also incorporated into 6FDA-DAM:DABA(4:1) (6FDA: 2,2-bis (3,4-carboxyphenyl) hexafluoropropane dianhydride and DAM: diaminomesitylene) to form the ZIF-8/6FDA-DAM:DABA(4:1) (20 wt% ZIF-8) dense films for CO_2 recovery from post-combustion flue gas streams. Good adhesion between the ZIF-8 and the 6FDA-DAM:DABA (4:1) matrix was observed. The dense film composites had a CO_2 permeability of 550 Barrers and a CO_2/N_2 selectivity of 19 at 35 ^{o}C. [108] ZIF-8/6FDA-DAM mixed matrix dense membranes were formed with 6FDA-DAM and 200 nm ZIF-8 particles. SEM imaging showed generally good adhesion between the ZIF-8 and 6FDA-DAM without the need for surface-treating ZIF-8. Pure gas permeation showed significantly enhanced C_3H_6/C_3H_8 separation performance over the pure 6FDA-DAM membrane performance. A C_3H_6 permeability of 56.2 Barrer and C_3H_6/C_3H_8 ideal selectivity of 31.0 were found in ZIF-8/6FDA-DAM mixed matrix membrane with 48.0 wt% ZIF-8 loading, which were 258% and 150% higher than those for the pure 6FDA-DAM

 This journal is © The Royal Society of Chemistry [year]

membrane, respectively.[109] Permeation properties of ZIF-8 were back-calculated using the Maxwell model, which led to a C_3H_6 permeability of 277 Barrer and C_3H_6/C_3H_8 ideal selectivity of 122. These results suggested that this polymer/ZIF-8 pair has the potential for application in reducing the energy intensity of C_3H_6/C_3H_8 separation process. [109]

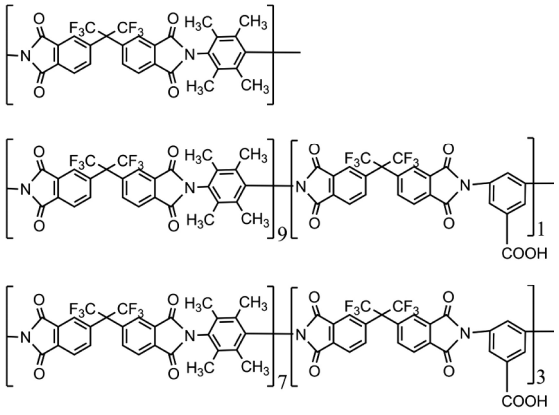

Fig. 18. Chemical structure of co-polyimides. Top: 6FDA-Durene polyimide, middle: 6FDA-Durene/DABA (9/1) co-polyimide, and bottom: 6FDA-Durene/DABA (7/3) co-polyimide. Reprinted with permission from ref. 107. Copyright 2013 Elsevier.

Bae et al. prepared ZIF-90 crystals with submicrometer and 2 µm sizes by a nonsolvent-induced crystallization technique, and incorporated them in 6FDA-DAM poly(imide) and two commercially available poly(imide)s (Ultem® 1000 (SABIC) and Matrimid® 5218 (Vantico)) to form the mixed matrix membranes.[110] For ZIF-90/6FDA-DAM membrane with 15 wt% ZIF-90, the highest CO_2 permeability was 720 barrer with a CO_2/CH_4 separation factor of 37 in a 1:1 CO_2: CH_4 mixture; this membrane showed much better performance than the pure 6FDA-DAM membrane (CO_2 permeability of 390 and CO_2/CH_4 separation factor of 24).[110] Nanocrystals of ZIF-90 were synthesized at room temperature through a novel procedure and incorporated into PBI for hydrogen purification. The derived ZIF-90/PBI nanocomposite membranes exhibited homogeneous particle dispersion and fine particle–polymer adhesion, as well as excellent hydrogen purification performance at various testing conditions. The 45/55 (w/w) ZIF-90/PBI membrane with the highest ZIF-90 volume loading of up to 50.9 vol% possessed the best ideal H_2/CO_2 separation performance with a moderate H_2 permeability of 24.5 Barrers and a high H_2/CO_2 ideal selectivity of 25.0 at 35 ^oC. The membrane also showed promoted gas separation performance during mixed gas tests at 180 ^oC with an H_2 permeability of 226.9 Barrers and an H_2/CO_2 separation factor of 13.3 that surpasses the latest Robeson upper bound for H_2/CO_2 separation.[111] ZIF-7 nanocrystals with sizes of 30-35 nm were incorporated into commercially available poly (amide-b-ethylene oxide) (Pebaxs 1657).[112] The performance of the composite membrane was characterized by single gas permeation measurement of CO_2, N_2 and CH_4. Both permeability and gas selectivity (CO_2/N_2 up to 97 and CO_2/CH_4 up to 30) was increased at a low ZIF-7 loading (8 wt%). The CO_2/CH_4 ideal selectivity was further increased to 44 with the filler loading of 34 wt%, but the permeability was reduced compared to the pure Pebaxs 1657 membrane. The membrane thickness of the 34 wt% ZIF-7 loading membrane was ~1 µm. Polymer chain rigidification at high filler loading was likely the reason for the reduced permeability. Overall, the ZIF-7/Pebaxs mixed matrix membranes showed a high performance for CO_2 separation from methane and other gas streams. [112]

To improve gas selectivity, surface cross-linking was performed on mixed matrix membranes containing 33.3 wt% ZIF-8 filler in 6FDA-durene polyimide, by exposure to ethylenediamine (EDA) vapor for 40 min (Fig. 19). Adding 33.3 wt% loading of nanocrystalline ZIF-8 to 6FDA-durene resulted in approximately a 400% increase in hydrogen and oxygen permeabilities. After the MMM was reacted with EDA vapor, a10 µm thick cross-linked skin on either side of the 70 µm thick membrane was observed. EDA cross-linking rendered ~10-fold increases in gas selectivities with respect to 6FDA-durene. The observed selectivities for the cross-linked MMM for H_2/CO_2, H_2/N_2,H_2/CH_4, and O_2/N_2 separations were 12, 141, 203, and 8.5, respectively, with corresponding hydrogen and oxygen permeabilities of 283.4 and 16.9 Barrers.[113]

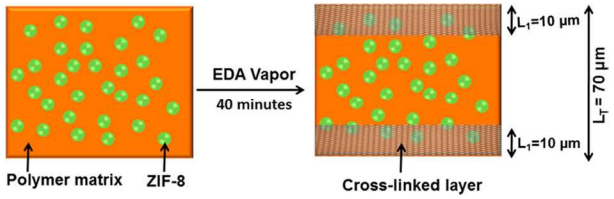

Fig. 19. Schematic representation of the formation of the cross-linked skin in 33.3 wt % ZIF-8/6FDA-durene MMM upon reaction with EDA vapor. Reprinted with permission from ref. 113. Copyright 2013 American Chemical Society.

Ionic liquid was also used to prepare mixed matrix membranes. ZIF-8 nanoparticles were incorporated in miscible ionic liquid blend systems for natural gas sweetening and post-combustion CO_2 capture. The miscible blend systems consist of a polymerizable room temperature ionic liquid (poly(RTIL)) and a "free" room temperature ionic liquids (RTILs). Experimental results showed that the free ionic liquids were miscible with poly(RTIL), while ZIF-8 were uniformly dispersed in the MMMs. The presence of ZIF-8 nanoparticles in the MMMs considerably improved gas permeability without much scarifying CO_2/N_2 and CO_2/CH_4 selectivities as compared to their poly(RTIL)/RTIL counterparts. The ZIF-8/P[vbim][NTf_2]/[emim][$B(CN)_4$] (poly(RTIL)= P[vbim][NTf_2]: 1-vinyl-3-butyl imidazolium-bis (trifluoromethyl-sulfonyl) imidate ; RTILs= [emim][$B(CN)_4$]: 1-ethyl-3-methylimidazolium tetracyanoborate) system with 25.8 wt% ZIF-8 exhibited impressive performance for post-combustion CO_2/N_2 (50/50 mol%) separation. It had a CO_2 permeability of 906.4 barrer and a CO_2/N_2 selectivity of 21 at 35 ^oC and 3.5 bar.

3.2. Symmetrical dense composite membrane for pervaporation

ZIF-8 nanoparticles exhibited exceptional adsorption selectivity and capacity toward isobutanol molecules, and showed a reversible gate-opening effect upon variation of the isobutanol pressure or temperature.[114] Freshly synthesized ZIF-8 nanoparticles were incorporated into polymethylphenylsiloxane (PMPS) to fabricate the ZIF-8/PMPS organophilic pervaporation membranes. The ZIF-8-PMPS membrane (W_{ZIF-8}: W_{PMPS}=0.10)

showed a very promising performance for recovering bio-alcohols from dilute aqueous solution. For pervaporation recovery of isobutanol from aqueous 1.0-3.0 wt% solutions at 80 °C, the separation factor of isobutanol over H_2O was of 34.9-40.1. Besides isobutanol, the ZIF-8/PMPS membrane exhibited higher selectivity and productivity for recovering other bio-alcohols from water compared with the pure PMPS membrane (Fig. 20). The pervaporation performance increases with the carbon number of the alcohols because of the increased adsorption selectivity and capacity. The decrease in separation factor and permeability for *n*-pentanol is characteristic of the interplay of adsorption and diffusion effects. However, ZIF-7/PMPS membrane prepared by the same procedure showed a lower separation factor and a lower isobutanol permeance compared with the ZIF-8/PMPS membrane due to the insignificant isobutanol adsorption of the ZIF-7 nanoparticles.[114] ZIF-8 nanocrystals with improved hydrothermal stability were achieved via a shell-ligand-exchange-reaction using 5,6-dimethylbenzimidazole (DMBIM) as the stabilizer, and they were incorporated into PMPS by the same research group for pervaporation recovery of isobutanol from water. Compared with the ZIF-8/PMPS membrane, the DMBIM stabilized ZIF-8/PMPS exhibited improved selectivity towards isobutanol while keeping the isobutanol flux constant.[115] The ZIF-8/PMPS membrane was also fabricated on a hierarchically ordered stainless-steel-mesh (HOSSM) employing a novel "Plugging-Filling" method.[116] The membrane exhibited the highest pervaporation separation index (separation factor 53.3 and total flux 0.90 kg m^{-2} h^{-1}) and excellent stability in a test of more than 120 h at 80 °C for recovery of furfural (1.0 wt%) from water. This very high performance should be attributed to the exceptional adsorption selectivity and capacity of ZIF-8 toward furfural molecules (450 mg g^{-1} for ZIF-8 nanoparticles) and the effects of space restriction and physical cross-linking of the HOSSM.[116]

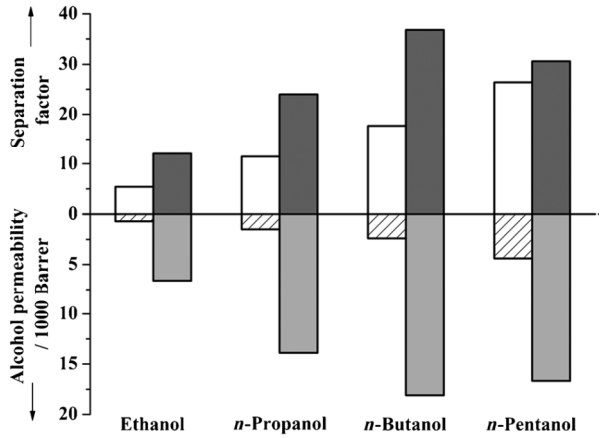

Fig. 20. Separation factor and alcohol permeability of PMPS (open and line filled columns) and ZIF-8-PMPS (gray and light gray columns) membranes for aqueous solutions of C_2-C_5 alcohols (1.0 wt% alcohols, 80 °C). Reprinted with permission from ref. 114. Copyright 2011 John Wiley & Sons, Inc.

ZIF-8/PBI mixed matrix membranes with a uniform dense structure have been prepared for pervaporation dehydration of ethanol, isopropanol (IPA) and butanol. As-synthesized ZIF-8 particles, with sizes smaller than 50 nm, were dispersed in the PBI phase directly with a loading ranging from12 wt% to 58 wt%. Pervaporation test data showed that the water permeability of ZIF-8/PBI (1:1) composite membranes was about one order of magnitude higher than the original PBI membrane (14,000-22,000 vs. 1200-2300 Barrer) (Fig. 21).[117] The degrees of membrane swelling after immersing in alcohols and water followed the order of ethanol > methanol > water > n-butanol. Addition of ZIF-8 particles into PBI membranes suppressed the ethanol-, methanol- and water-induced PBI swelling. The water-induced swelling was subdued most severely because of the hydrophobic nature and rigid structure of ZIF-8 particles, while the n-butanol-induced swelling was enhanced owing to a greater free volume in the ZIF-8/PBI membrane.[118] ZIF-7 crystal particles were successfully incorporated into chitosan (CS) membranes to form ZIF-7/CS mixed-matrix membranes. Glutaraldehyde (GA) cross-linkers were used to increase the linking of the chitosan chains. In the H_2O/ethanol pervaporation test, the separation efficiency of the membrane with 5 wt% ZIF-7 was 19 times higher than that of the pristine CS membranes because of the rigidified polymer chain of the MMMs. The highest H_2O/ethanol separation factor was 2812 with a total flux of 322 g m^{-2} h^{-1}.[119]

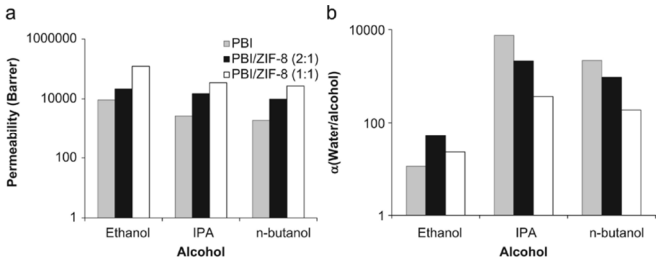

Fig. 21. (a) Water permeability and (b) selectivity for water of PBI/ZIF-8 MMMs for pervaporation dehydration of alcohols (Feed: alcohol/water 85/15wt% at 60 °C). Reprinted with permission from ref. 117. Copyright 2012 Elsevier.

New mixed matrix membranes were prepared by incorporating ZIF-71 particles into polyether-block-amide (PEBA) for biobutanol recovery from acetone-butanol-ethanol (ABE) fermentation broth by pervaporation. The incorporation of ZIF-71 particles into PEBA significantly improved the n-butanol separation performance of the membranes. A simultaneous enhancement in both separation factor and flux was achieved by optimizing the amount of ZIF-71. The MMMs with 20 wt% loading showed high total flux of 520.2 g m^{-2} h^{-1} and n-butanol separation factor of 18.8 at 37 °C in model ABE solution. In addition, the membrane exhibited stable performance in the real ABE fermentation broth for 100 h with average total flux of 447.9 g m^{-2} $h^{-1}$and n-butanol separation factor of 18.4 (Fig. 22).[120] Hua et al. synthesized ZIF-90 nanoparticles with an average particle size of 55 nm and embedded them into P84 polymeric membranes with excellent dispersion for the dehydration of isopropanol (IPA)/water mixture via pervaporation.[121] The effects of ZIF-90 loading as well as feed temperature on pervaporation performance of the mixed matrix membranes were systematically investigated. The flux of MMMs increased with increasing ZIF-90 loading due to the enhanced fractional free volume; the separation factor of water/IPA could be maintained at 5432 when the ZIF-90 loading was less than 20 wt%, but reduced to 385 when the ZIF-90 loading was 30 wt%. The application of

This journal is © The Royal Society of Chemistry [year]

sulfonated polyethersulfone (SPES) as a primer to ZIF-90 nanoparticles before fabricating 30 wt% ZIF-90 MMM resulted in an increase in the separation factor from 385 to 5668 due to the enhanced affinity between ZIF-90 particles and P84 as well as the preferential sorption of water over IPA. The best MMM showed a flux of 109 g m^{-2} h^{-1} and a separation factor of 5668 at 60 °C.[121]

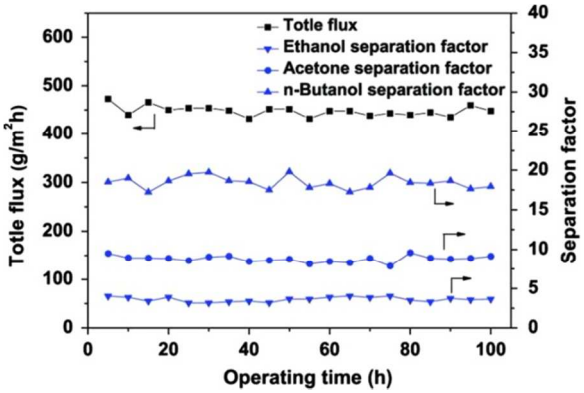

Fig. 22. Stability of ZIF-71/PEBA MMMs with 20 wt% loading in acetone-butanol-ethanol fermentation broth: total flux and separation factor of acetone, n-butanol and ethanol. Reprinted with permission from ref. 120. Copyright 2013 Elsevier.

3.3. Asymmetric composite membranes

Although many symmetric dense films studies have been reported, there have been few studies on preparation of asymmetric composite hollow fibers with ZIFs. Asymmetric composite membranes composed of a thin dense selective layer and a macroporous supporting layer usually have much higher flux than symmetric membranes, and hence they are highly desirable for practical applications. Dai et al. reported the first successful production of mixed matrix asymmetric hollow fiber membranes containing ZIF-8 fillers.[122] ZIF-8 nanoparticles with a size of ca. 200 nm were incorporated into a polyetherimide (Ultem® 1000) matrix and produced dual-layer asymmetric hollow fiber membranes via the dry jet-wet quench method. The hollow fibers were post-treated with a 2 wt% high molecular weight polydimethylsiloxane solution in heptane to seal any pinhole defects in the selective skin layer. The outer separating layer of these composite fibers contained 13 wt% (17 vol%) of ZIF-8 filler. The ZIF-8/Ultem® hollow fibers showed increased CO_2 permeance of 18 GPU with an ideal selectivity of 44, which was as high as 20% over pure polymer (permeance: 11; ideal selectivity: 36). A mixed gas (CO_2/N_2, 20/80) selectivity of 32 was achieved in these hollow fiber membranes at 25 °C.[122] ZIF-8/PBI composite dual-layer hollow fiber membranes were prepared, and they showed promising hydrogen separation properties at high temperatures.[103] Defect-free ZIF-8-PBI/Matrimid dual-layer hollow fibers were successfully fabricated, without post-annealing and coating, by optimizing ZIF-8 nanoparticle loadings, spinning conditions, and solvent-exchange procedures. Two types of hollow fibers targeted at either high H_2/CO_2 selectivity or high H_2 permeance were developed: the first type of fibers with a medium H_2 permeance of 2.16×10^{-8} mol m^{-2} s^{-1} pa^{-1} at 180 °C and a high H_2/CO_2 selectivity of 12.3, and the second type of fibers with a high H_2 permeance of 6.77 $\times10^{-8}$ mol m^{-2} s^{-1} pa^{-1} at 180 °C and a medium H_2/CO_2 selectivity of 7.7 for the separation of H_2/CO_2 (50:50) mixed gas.[103]

The non-network polydioxane PIM-1[123] performs at the latest upper bound for a number of important gas pairs as the macromolecular PIM-1 traps free volume in the solid state. Self-supported ZIF-8/PIM-1 films with ZIF-8 contents up to 43 vol% were prepared. Permeability coefficients were determined for the following set of gases: He, H_2, O_2, N_2, CO_2, and CH_4. For "as-cast" films, an increase in ZIF-8 loading resulted in increases in the permeability and diffusion coefficients as well as in the ideal selectivity of H_2/N_2, H_2/CH_4, He/N_2, O_2/N_2 and CO_2/CH_4. For all ZIF-8 contents studied, the permeability was enhanced by treatment with ethanol. The permeability of H_2, He, O_2, N_2, CO_2 and CH_4 was 14430, 5990, 5810, 1760, 19350 and 2660 Barrers, respectively for ethanol-treated ZIF-8/PIM-1 membrane (43 vol% ZIF-8).[124] Data points on several Robeson diagrams are located above the latest upper bound.

Table 4 Summary of mixed matrix membranes incorporated with ZIFs for gas separation and liquid separation via pervaporation.

Polymers	ZIFs	Applications	Performance	Ref.
Matrimid®	ZIF-8	Gas separation	CO_2/CH_4 ideal selectivity: 124.89±72.22, and separation factor: 89.15±5.92 (10/90, CO_2/CH_4) (50% ZIF-8)	99
Matrimid®	ZIF-8	Gas separation	Ideal selectivity H_2/CH_4 (137), CO_2/CH_4 (35.8) (20% ZIF-8)	100
Matrimid®	ZIF-8	Gas separation	CO_2/CH_4 ideal selectivity ~39 (25% ZIF-8)	101
Polybenzimidazole (PBI)	ZIF-7	Gas separation	H_2/CO_2 ideal selectivity up to 12.3, H_2 permeability: 105.4 barrer (up to 50% ZIF-7)	102,103
PBI	ZIF-8	Gas separation	H_2/CO_2 ideal selectivity 12.3 at 230 °C, H_2 permeability: 2014.8 barrer (60% ZIF-8)	104
PPEES	ZIF-8	Gas separation	Ideal selectivity O_2/N_2 (6.2), H_2/N_2 (70) (30% ZIF-8)	106
6FDA-Durene/DABA(9/1)	ZIF-8	Gas separation	C_3H_6/C_3H_8 ideal selectivity: 27.38, separation factor: 19.61 (40% ZIF-8)	107
6FDA-DAM/DABA (4/1)	ZIF-8	Gas separation	CO_2/N_2 ideal selectivity: 19, CO_2 permeability 550 barrer (20% ZIF-8)	108
6FDA-DMA	ZIF-8	Gas separation	C_3H_6/C_3H_8 ideal selectivity 31 (48% ZIF-8)	109
6FDA-DAM	ZIF-90	Gas separation	CO_2/CH_4 separation factor 37 (1:1 CO_2/CH_4), CO_2 permeability: 720 barrer (15% ZIF-90)	110
PBI	ZIF-90	Gas separation	H_2/CO_2 ideal selectivity 25, H_2 permeability 24.5 (45% ZIF-	111

			90)	
Pebaxs® 1657	ZIF-7	Gas separation	CO_2/CH_4 ideal selectivity 44. (34% ZIF-7)	112
6FDA-Durene	ZIF-8	Gas separation	Ideal selectivity H_2/CH_4 (203), O_2/N_2 (8.5) (33.3% ZIF-8)	113
Ionic liquid	ZIF-8	Gas separation	CO_2/N_2 separation factor 21 (1:1 CO_2/N_2), CO_2 permeability 906.4 barrer (25.8% ZIF-8)	125
Polymethylphenylsiloxane (PMPS)	ZIF-8	Organophilic pervaporation	Separation factor isobutanol over water 34.9-40.1 (10% ZIF-8)	114
PMPS	ZIF-8	Organophilic pervaporation	Furfural separation factor 53.3, total flux 0.9 kg m^{-2} h^{-1} (45% ZIF-8)	116
PBI	ZIF-8	Pervaporation dehydration	Water permeability: one order higher than the original PBI membrane (58.7% ZIF-8)	117
Chitosan	ZIF-7	pervaporation	H_2O/ethanol separation factor: 2812, total flux 322 g m^{-2} h^{-1} (5% ZIF-7)	119
Polyether-block-amide	ZIF-71	Pervaporation: biobutanol recovery	n-butanol separation factor 18.8 (acetone-butanol-ethanol fermentation system), total flux: 520.2 g m^{-2} h^{-1} (20% ZIF-71)	120
P84	ZIF-90	Pervaporation	Dehydration of isopropanol/water mixture. Total flux of 109 g m^{-2} h^{-1} and a separation factor of 5668 at 60 °C.	121
polyetherimide (Ultem® 1000)	ZIF-8	Gas separation	CO_2/N_2 ideal selectivity: 44; separation factor: 32 (CO_2/N_2, 20/80)	122
PBI	ZIF-8	Gas separation	High H_2/CO_2 separation factor (12.3) or high H_2 permeance (1:1 H_2/CO_2)	103
PIM-1	ZIF-8	Gas separation	High permeability: single gases H_2, He, O_2, N_2, CO_2 and CH_4	124
Matrimid®	ZIF-8	Gas separation	CO_2/CH_4 separation factor 32 (CO_2/CH_4 35/65)	126

4. ZIF films for microelectronics

Apart from the selective separation membranes, ZIF films have also been fabricated as sensors and insulators for microelectronics. Many ZIFs show excellent selective adsorption properties and can be used for sensing chemicals whereas the large microporosity and hydrophobicity of ZIFs are attractive features for use as insulators with low dielectric constants. In these applications, growth of high-quality ZIFs films on dense substrates with tunable thickness, and patterning of ZIF films on substrates are often required.

By using the drain and capillary regimes involved in the dip-coating process, Demessenc et al. prepared ZIF-8 films on silicon wafer, and the thickness of the films could be tuned from 40 nm to 1 μm.[127] The high optical-quality thin films showed a dual hierarchical porous structure from the micropores of ZIF-8 and the mesoporous interparticular voids. ZIF-8 crystals are strongly hydrophobic due to the presence of methyl groups positioned at the entrance of the pore opening,[128] and organic molecules such as alcohols, tetrahydrofuran and hydrocarbons tend to be more easily adsorbed. These thin films exhibited selective adsorption properties for organic vapors versus water, which could make those high optical thin films good candidates for vapor sensors.[127] Lu et al. prepared ZIF-8 thin film-based Fabry-Pérot device as a selective sensor for chemical vapors and gases. The preparation of the ZIF-8 thin film and a series of ZIF-8 thin films of various thicknesses grown on silicon substrates are shown in Fig. 23. The ZIF-8 sensor displayed some chemical selectivity. For example, linear n-hexane was readily sensed, but the cyclohexane was not. Exposure the ZIF-8 films to the vapor above ethanol/water mixtures of various ethanol contents gave rise to ethanol-concentration-dependent responses, with the sensor response saturating at ca. 40% ethanol.[129]

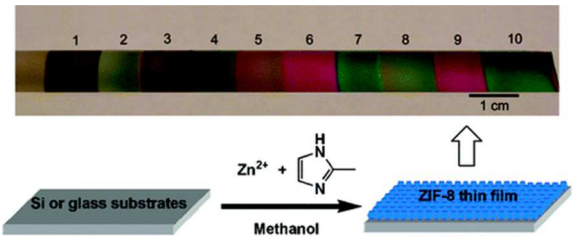

Fig. 23 . Photograph of a series of ZIF-8 films of various thicknesses grown on silicon substrates, and their preparation procedure. Reprinted with permission from ref. 129. Copyright 2010 American Chemical Society.

Patterned ZIF-8 thin films were generated by using standard photolithography or via selective growth with the aid of microcontact printing (Fig. 24). For the latter method, the surface modification of silicon substrates with hydrophobic silane self-assembled monolayer (CH_3-terminated SAMs) was done by soaking the pre-cleaned substrates in a 5% solution (v/v) of octadecyltrimethoxy silane in toluene with 0.5% n-butylamine. The alternate chemical deposition (of ZIF-8) and physical deposition (of metallic materials) allow the insertion of metal layers in the ZIF-8 film that could serve as multifunctional chemical sensors for vapors and gases.[130] A new, versatile method for patterning ZIF surfaces by a top-down X-ray lithographic approach was developed by Dimitrakakis et al. that may reduce the reliance on surface chemistry and reaction kinetics optimization for producing patterned materials.[131] This

This journal is © The Royal Society of Chemistry [year]

has been achieved through control of the irradiation conditions to ensure that the crystallinity and the adsorption capacities of ZIF-9 have been preserved, allowing this approach to potentially be applied for gas separation, sensing or transport by adapting the method to a variety of framework materials and substrates.

ZIF-8 films were deposited on silicon wafers and characterized to assess their potential as future insulators (low-κ dielectrics) in microelectronics. The dielectric constant was measured by impedance analysis at different frequencies and temperatures, indicating that κ was only 2.33 (±0.05) at 100 kHz, a result of low polarizability and density in the films. Intensity voltage curves showed that the leakage current was only 10^{-8} A cm^2 at 1 MV cm^{-1}, and the breakdown voltage was above 2 MV cm^{-1}. ZIF-8 films have the effective κ value necessary for future chips, good mechanical properties, hydrophobicity, and they outperform other low-κ candidates in terms of pore entrance size and hydrophobicity.[132]

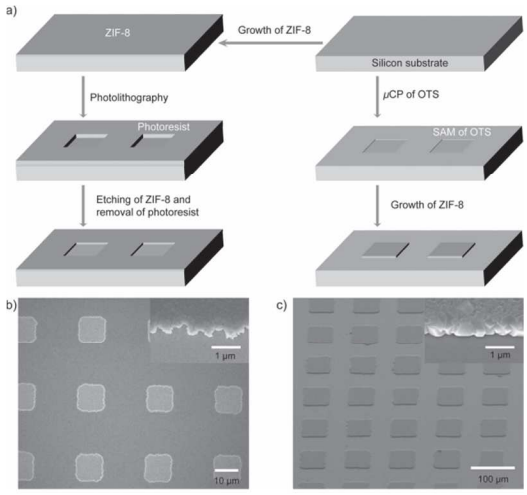

Fig. 24. a) Schematic diagram of the processes for patterning ZIF-8 thin films via photolithography (left) and microcontact printing (μCP) (right). Typical SEM images of patterns in ZIF-8 thin films obtained by means of b) photolithography and c) microcontact printing. Insets in b) and c) show the high-magnification SEM images of the edges of pattern features. Reprinted with permission from ref. 130. Copyright 2012 John Wiley & Sons, Inc.

5. Conclusions and perspectives

Recent years have witnessed a great deal of progress made in the development of zeolitic imidazolate framework membranes and films for separation applications and functional microelectronic devices, and fundamental understanding of the membrane formation and gas transport processes.

To date, ZIF membranes/films have been prepared by various methods including direct synthesis, secondary growth with pre-seeding of the substrate, surface functionalization with covalent linkers, imidazolate deposition, precursor infiltration, reactive seeding method, and contra (counter) diffusion method. However, due to complex ZIF nucleation and growth processes, it is hard to directly correlate the preparation method with the membrane properties. In general, repetitive growth including secondary growth tends to reduce defects of ZIF membranes. A wide range of parameters should be considered in the fabrication of ZIF membranes, including the surface properties of the substrates, and the crystallization behavior of individual ZIFs. Therefore, a combination of different methods such as surface functionalization, secondary seeded growth and post-functionalization may be required to achieve optimal membrane structures and performances in some ZIF systems.

Studies have shown that ZIF crystals are attractive additives for the fabrication of polymer-based composite membranes (known as mixed matrix membranes), including symmetrical dense composite membranes and asymmetrical composite membranes with relatively high loadings of ZIFs due to good compatibility between ZIFs and polymers. The incorporation of ZIF particles into a polymer increases the free volume of polymer, and thus enhances the solubility and diffusivity of the targeted components.

In terms of applications, both ZIF membranes and ZIF/polymer composite membranes have been widely studied for energy and environment related separations such as hydrogen separation, CO_2 capture, light hydrocarbons separation, and liquid mixture separation (dehydration and organophilic pervaporation). However, the flexible property of imidazolate linkers of ZIFs induces the complex pore changes, such as pore size increase[133] and gate opening[87] under certain conditions, adding more complexity of ZIF membranes in gas separation and liquid separation.

ZIF films have been fabricated as sensors and insulators for microelectronics. The easy synthesis of ZIF films and the structure versatility of ZIFs may offer some interesting properties for components in future generation microelectronics, but more research is needed to explore real potential of ZIFs over their zeolite counterparts in this area.[6]

Among many different types of ZIFs studied, ZIF-8 has been the most extensively studied ZIF due to its good thermal and chemical stability, and easy synthesis. A few other types of ZIFs also deserve more attention. ZIF-11 with RHO topology possesses larger cages connected through small apertures, and also exhibits exceptional thermal and chemical resistance to water and organic solvents.[2] The molecular simulation revealed that ZIF-11 has the potential to meet industrial requirements for H_2/CO_2 and H_2/N_2 separations, a critical operation for pre-combustion carbon capture.[134] However, the synthesis of ZIF-11 at low cost and low environmental impact is yet to be realized.[135] Theoretical modelling suggested that ZIF-77 may be good for natural gas purification (CO_2/CH_4) while ZIF-71 may be an excellent candidate for air separation for oxy-combustion (O_2/N_2).[134] Furthermore, ZIF-8 was recently used as a CO_2 adsorbent in aqueous solution, effectively enhancing the photocatalytic CO_2 reduction reaction into liquid fuels.[136] Since many ZIFs are stable in water, it is worthy of research efforts in investigating their potential use as selective adsorbents in photocatalytic membrane reactors[137,138] and as an additive to modify desalination membranes.[139,140]

Despite ZIF/polymer mixed matrix membranes have been demonstrated for their potential for gas separations such as CO_2 capture from flue gas,[122] their structures and separation performances still need to be further optimized for large scale practical applications. Significant efforts are required to synthesize different types of ZIF nanoparticles with sizes smaller than 100 nm in order to investigate the effect of particle size on

membrane properties. In addition, since it is possible to synthesize ZIF nanoflakes[141] and nanorods,[50] it would be interesting to investigate how the ZIF particle shape affects membrane structure and separation properties as observed in the zeolite/polymer composite membranes.[142,143]

Due to the structure diversity of ZIFs, a designed and tunable organic adsorption could be obtained and the organophilic pervaporation could be expected by using ZIF membranes or ZIF/polymer composite membranes.[84,120] More studies on long-term stability of ZIF composite membranes under different operational environments such as organic solvents in pervaporation, and gas mixtures containing water and organic vapor in high temperature are required. The scale up of ZIF/polymer mixed matrix membranes is quite straightforward since their fabrication processes are primarily based on well-established polymer membrane technologies. But it would be challenging to fabricate ZIF membranes on a large scale, and a major breakthrough is needed to reliably grow defect-free membranes and eliminate grain boundary defects.[144] Given strong interest in ZIFs in the research community, new concepts and techniques for synthesis of high-quality ZIF membranes and films will continue to emerge in the future.

Acknowledgements

J.Y. thanks Monash University for a Monash Fellowship. H.W. acknowledges the support of the Australian Research Council through a Future Fellowship (FT100100192).

Notes and references

Department of Chemical Engineering, Monash University, Clayton, Victoria 3800, Australia.
Tel: +61 3 9905 9621. Email: jianfeng.yao@monash.edu (JY); huanting.wang@monash.edu (HW).

Reference

1. A. Phan, C. J. Doonan, F. J. Uribe-Romo, C. B. Knobler, M. O'Keeffe and O. M. Yaghi, *Acc. Chem. Res.*, 2010, **43**, 58-67.
2. K. S. Park, Z. Ni, A. P. Cote, J. Y. Choi, R. D. Huang, F. J. Uribe-Romo, H. K. Chae, M. O'Keeffe and O. M. Yaghi, *Proc. Natl. Acad. Sci. U. S. A.*, 2006, **103**, 10186-10191.
3. S. L. James, *Chem. Soc. Rev.*, 2003, **32**, 276-288.
4. M. Eddaoudi, D. B. Moler, H. L. Li, B. L. Chen, T. M. Reineke, M. O'Keeffe and O. M. Yaghi, *Acc. Chem. Res.*, 2001, **34**, 319-330.
5. A. Betard and R. A. Fischer, *Chem. Rev.*, 2012, **112**, 1055-1083.
6. C. M. Lew, R. Cai and Y. S. Yan, *Acc. Chem. Res.*, 2010, **43**, 210-219.
7. M. A. Snyder and M. Tsapatsis, *Angew. Chem. Int. Edit.*, 2007, **46**, 7560-7573.
8. D. Zacher, O. Shekhah, C. Woll and R. A. Fischer, *Chem. Soc. Rev.*, 2009, **38**, 1418-1429.
9. D. Bradshaw, A. Garai and J. Huo, *Chem. Soc. Rev.*, 2012, **41**, 2344-2381.
10. O. Shekhah, J. Liu, R. A. Fischer and C. Woll, *Chem. Soc. Rev.*, 2011, **40**, 1081-1106.
11. M. Shah, M. C. McCarthy, S. Sachdeva, A. K. Lee and H. K. Jeong, *Ind. Eng. Chem. Res.*, 2012, **51**, 2179-2199.
12. J. R. Li, Y. G. Ma, M. C. McCarthy, J. Sculley, J. M. Yu, H. K. Jeong, P. B. Balbuena and H. C. Zhou, *Coord. Chem. Rev.*, 2011, **255**, 1791-1823.
13. H. Hayashi, A. P. Cote, H. Furukawa, M. O'Keeffe and O. M. Yaghi, *Nat. Mater.*, 2007, **6**, 501-506.
14. F. Wang, Y. X. Tan, H. Yang, H. X. Zhang, Y. Kang and J. Zhang, *Chem. Commun.*, 2011, **47**, 5828-5830.
15. X. C. Huang, J. P. Zhang and X. M. Chen, *Chin. Sci. Bull.*, 2003, **48**, 1531-1534.
16. J. Caro and M. Noack, *Microporous Mesoporous Mater.*, 2008, **115**, 215-233.
17. J. Caro, M. Noack, P. Kolsch and R. Schafer, *Microporous Mesoporous Mater.*, 2000, **38**, 3-24.
18. A. Tavolaro and E. Drioli, *Adv. Mater.*, 1999, **11**, 975-996.
19. S. Basu, A. L. Khan, A. Cano-Odena, C. Q. Liu and I. F. J. Vankelecom, *Chem. Soc. Rev.*, 2010, **39**, 750-768.
20. L. Y. Jiang, Y. Wang, T. S. Chung, X. Y. Qiao and J. Y. Lai, *Prog. Polym. Sci.*, 2009, **34**, 1135-1160.
21. J. G. Wijmans and R. W. Baker, *J. Membr. Sci.*, 1995, **107**, 1-21.
22. X. C. Huang, Y. Y. Lin, J. P. Zhang and X. M. Chen, *Angew. Chem. Int. Edit.*, 2006, **45**, 1557-1559.
23. R. Banerjee, A. Phan, B. Wang, C. Knobler, H. Furukawa, M. O'Keeffe and O. M. Yaghi, *Science*, 2008, **319**, 939-943.
24. R. Banerjee, H. Furukawa, D. Britt, C. Knobler, M. O'Keeffe and O. M. Yaghi, *J. Am. Chem. Soc.*, 2009, **131**, 3875-3877.
25. W. Morris, C. J. Doonan, H. Furukawa, R. Banerjee and O. M. Yaghi, *J. Am. Chem. Soc.*, 2008, **130**, 12626-12627.
26. B. Wang, A. P. Cote, H. Furukawa, M. O'Keeffe and O. M. Yaghi, *Nature*, 2008, **453**, 207-U206.
27. S. Aguado, C. H. Nicolas, V. Moizan-Basle, C. Nieto, H. Amrouche, N. Bats, N. Audebrand and D. Farrusseng, *New J. Chem.*, 2011, **35**, 41-44.
28. C. J. Zhang, Y. L. Xiao, D. H. Liu, Q. Y. Yang and C. L. Zhong, *Chem. Commun.*, 2013, **49**, 600-602.
29. H. Bux, F. Y. Liang, Y. S. Li, J. Cravillon, M. Wiebcke and J. Caro, *J. Am. Chem. Soc.*, 2009, **131**, 16000-16001.
30. H. Bux, C. Chmelik, J. M. van Baten, R. Krishna and J. Caro, *Adv. Mater.*, 2010, **22**, 4741-4743.
31. E. Haldoupis, S. Nair and D. S. Sholl, *J. Am. Chem. Soc.*, 2010, **132**, 7528-7539.
32. H. Bux, C. Chmelik, R. Krishna and J. Caro, *J. Membr. Sci.*, 2011, **369**, 284-289.
33. M. Shah, H. T. Kwon, V. Tran, S. Sachdeva and H. K. Jeong, *Microporous Mesoporous Mater.*, 2013, **165**, 63-69.
34. Y. Y. Liu, E. P. Hu, E. A. Khan and Z. P. Lai, *J. Membr. Sci.*, 2010, **353**, 36-40.
35. S. R. Venna and M. A. Carreon, *J. Am. Chem. Soc.*, 2010, **132**, 76-78.
36. H. Bux, A. Feldhoff, J. Cravillon, M. Wiebcke, Y. S. Li and J. Caro, *Chem. Mater.*, 2011, **23**, 2262-2269.
37. H. K. Jeong, J. Krohn, K. Sujaoti and M. Tsapatsis, *J. Am. Chem. Soc.*, 2002, **124**, 12966-12968.
38. S. H. Du, Y. G. Liu, L. Y. Kong, J. Zhang, H. O. Liu and X. F. Zhang, *J. Inorg. Mater.*, 2012, **27**, 1105-1111.
39. Y. C. Pan and Z. P. Lai, *Chem. Commun.*, 2011, **47**, 10275-10277.
40. Y. C. Pan, T. Li, G. Lestari and Z. P. Lai, *J. Membr. Sci.*, 2012, **390**, 93-98.
41. D. F. Liu, X. L. Ma, H. X. Xi and Y. S. Lin, *J. Membr. Sci.*, 2014, **451**, 85-93.
42. J. F. Yao, L. X. Li, W. H. B. Wong, C. Z. Tan, D. H. Dong and H. T. Wang, *Mater. Chem. Phys.*, 2013, **139**, 1003-1008.
43. G. S. Xu, J. F. Yao, K. Wang, L. He, P. A. Webley, C. S. Chen and H. T. Wang, *J. Membr. Sci.*, 2011, **385**, 187-193.
44. K. Tao, C. L. Kong and L. Chen, *Chem. Eng. J.*, 2013, **220**, 1-5.
45. Y. C. Pan, B. Wang and Z. P. Lai, *J. Membr. Sci.*, 2012, **421**, 292-298.
46. Y. S. Li, F. Y. Liang, H. Bux, A. Feldhoff, W. S. Yang and J. Caro, *Angew. Chem. Int. Edit.*, 2010, **49**, 548-551.
47. L. M. Robeson, *J. Membr. Sci.*, 2008, **320**, 390-400.
48. Y. S. Li, F. Y. Liang, H. G. Bux, W. S. Yang and J. Caro, *J. Membr. Sci.*, 2010, **354**, 48-54.
49. J. F. Yao, D. Li, K. Wang, L. He, G. S. Xu and H. T. Wang, *J. Nanosci. Nanotechnol.*, 2013, **13**, 1431-1434.
50. Y. S. Li, H. Bux, A. Feldhoff, G. L. Li, W. S. Yang and J. Caro, *Adv. Mater.*, 2010, **22**, 3322-3326.
51. Y. Y. Liu, G. F. Zeng, Y. C. Pan and Z. P. Lai, *J. Membr. Sci.*, 2011, **379**, 46-51.

 This journal is © The Royal Society of Chemistry [year]

52. O. Shekhah, R. Swaidan, Y. Belmabkhout, M. du Plessis, T. Jacobs, L. Barbour, I. Pinnau and M. Eddaoudi, *Chem. Commun.*, 2014, **50**, 2089-2092.
53. O. Shekhah and M. Eddaoudi, *Chem. Commun.*, 2013, **49**, 10079-10081.
54. J. F. Yao, D. H. Dong, D. Li, L. He, G. S. Xu and H. T. Wang, *Chem. Commun.*, 2011, **47**, 2559-2561.
55. P. S. Goh, A. F. Ismail, S. M. Sanip, B. C. Ng and M. Aziz, *Sep. Purif. Technol.*, 2011, **81**, 243-264.
56. L. Ge, W. Zhou, A. J. Du and Z. H. Zhu, *J. Phys. Chem. C*, 2012, **116**, 13264-13270.
57. W. B. Li, Z. H. Yang, G. L. Zhang, Z. Fan, Q. Meng, C. Shen and C. J. Gao, *J. Mater. Chem. A*, 2013.
58. D. Nagaraju, D. G. Bhagat, R. Banerjee and U. K. Kharul, *J. Mater. Chem. A*, 2013, **1**, 8828-8835.
59. A. J. Brown, J. R. Johnson, M. E. Lydon, W. J. Koros, C. W. Jones and S. Nair, *Angew. Chem. Int. Edit.*, 2012, **51**, 10615-10618.
60. M. R. Kosuri and W. J. Koros, *J. Membr. Sci.*, 2008, **320**, 65-72.
61. L. Ge, A. J. Du, M. Hou, V. Rudolph and Z. H. Zhu, *RSC Adv.*, 2012, **2**, 11793-11800.
62. L. Dumee, L. He, M. Hill, B. Zhu, M. Duke, J. Schutz, F. S. She, H. T. Wang, S. Gray, P. Hodgson and L. X. Kong, *J. Mater. Chem. A*, 2013, **1**, 9208-9214.
63. M. He, J. F. Yao, Z. X. Low, D. B. Yu, Y. Feng and H. T. Wang, *RSC Adv.*, 2014, **4**, 7634-7639.
64. A. S. Huang, H. Bux, F. Steinbach and J. Caro, *Angew. Chem. Int. Edit.*, 2010, **49**, 4958-4961.
65. A. S. Huang, W. Dou and J. Caro, *J. Am. Chem. Soc.*, 2010, **132**, 15562-15564.
66. A. S. Huang and J. Caro, *Angew. Chem. Int. Edit.*, 2011, **50**, 4979-4982.
67. A. S. Huang, N. Y. Wang, C. L. Kong and J. Caro, *Angew. Chem. Int. Edit.*, 2012, **51**, 10551-10555.
68. A. S. Huang, Y. F. Chen, N. Y. Wang, Z. Q. Hu, J. W. Jiang and J. Caro, *Chem. Commun.*, 2012, **48**, 10981-10983.
69. K. Huang, Z. Y. Dong, Q. Q. Li and W. Q. Jin, *Chem. Commun.*, 2013, **49**, 10326-10328.
70. M. C. McCarthy, V. Varela-Guerrero, G. V. Barnett and H. K. Jeong, *Langmuir*, 2010, **26**, 14636-14641.
71. K. Tao, L. J. Cao, Y. C. Lin, C. L. Kong and L. Chen, *J. Mater. Chem. A*, 2013, **1**, 13046-13049.
72. L. X. Li, J. F. Yao, R. Z. Chen, L. He, K. Wang and H. T. Wang, *Microporous Mesoporous Mater.*, 2013, **168**, 15-18.
73. X. L. Dong, K. Huang, S. N. Liu, R. F. Ren, W. Q. Jin and Y. S. Lin, *J. Mater. Chem.*, 2012, **22**, 19222-19227.
74. X. F. Zhang, Y. G. Liu, L. Y. Kong, H. O. Liu, J. S. Qiu, W. Han, L. T. Weng, K. L. Yeung and W. D. Zhu, *J. Mater. Chem. A*, 2013, **1**, 10635-10638.
75. M. He, J. F. Yao, L. X. Li, Z. X. Zhong, F. Y. Chen and H. T. Wang, *Microporous Mesoporous Mater.*, 2013, **179**, 10-16.
76. Z. Xie, J. H. Yang, J. Q. Wang, J. Bai, H. M. Yin, B. Yuan, J. M. Lu, Y. Zhang, L. Zhou and C. Y. Duan, *Chem. Commun.*, 2012, **48**, 5977-5979.
77. N. Hara, M. Yoshimune, H. Negishi, K. Haraya, S. Hara and T. Yamaguchi, *J. Membr. Sci.*, 2014, **450**, 215-223.
78. A. S. Huang, Q. Liu, N. Y. Wang and J. Caro, *Microporous Mesoporous Mater.*, 2014, **doi: 10.1016/j.micromeso.2013.09.025**.
79. K. Kida, K. Fujita, T. Shimada, S. Tanaka and Y. Miyake, *Dalton Trans.*, 2013, **42**, 11128-11135.
80. C. T. Hou, Q. Xu, J. Y. Peng, Z. P. Ji and X. Y. Hu, *ChemPhysChem*, 2013, **14**, 140-144.
81. L. L. Fan, M. Xue, Z. X. Kang, H. Li and S. L. Qiu, *J. Mater. Chem.*, 2012, **22**, 25272-25276.
82. R. Ostermann, J. Cravillon, C. Weidmann, M. Wiebcke and B. M. Smarsly, *Chem. Commun.*, 2011, **47**, 442-444.
83. Y. X. Hu, X. L. Dong, J. P. Nan, W. Q. Jin, X. M. Ren, N. P. Xu and Y. M. Lee, *Chem. Commun.*, 2011, **47**, 737-739.
84. X. L. Dong and Y. S. Lin, *Chem. Commun.*, 2013, **49**, 1196-1198.
85. L. L. Fan, M. Xue, Z. X. Kang, G. Y. Wei, L. Huang, J. S. Shang, D. L. Zhang and S. L. Qiu, *Microporous Mesoporous Mater.*, 2014, **doi: 10.1016/j.micromeso.2013.11.008**.
86. A. Kasik and Y. S. Lin, *Sep. Purif. Technol.*, 2014, **121**, 38-45.
87. L. Diestel, H. Bux, D. Wachsmuth and J. Caro, *Microporous Mesoporous Mater.*, 2012, **164**, 288-293.
88. H. T. Kwon and H.-K. Jeong, *J. Am. Chem. Soc.*, 2013, **135**, 10763-10768.
89. H. T. Kwon and H. K. Jeong, *Chem. Commun.*, 2013, **49**, 3854-3856.
90. S. K. Seshadri, H. M. Alsyouri and Y. S. Lin, *Microporous Mesoporous Mater.*, 2010, **129**, 228-237.
91. W. Xiao, J. H. Yang, J. M. Lu and J. Q. Wang, *J. Membr. Sci.*, 2009, **345**, 183-190.
92. H. M. Alsyouri, D. Li, Y. S. Lin, Z. Ye and S. P. Zhu, *J. Membr. Sci.*, 2006, **282**, 266-275.
93. H. B. T. Jeazet, C. Staudt and C. Janiak, *Dalton Trans.*, 2012, **41**, 14003-14027.
94. T. S. Chung, L. Y. Jiang, Y. Li and S. Kulprathipanja, *Prog. Polym. Sci.*, 2007, **32**, 483-507.
95. A. F. Ismail, P. S. Goh, S. M. Sanip and M. Aziz, *Sep. Purif. Technol.*, 2009, **70**, 12-26.
96. M. A. Aroon, A. F. Ismail, T. Matsuura and M. M. Montazer-Rahmati, *Sep. Purif. Technol.*, 2010, **75**, 229-242.
97. R. Mahajan, R. Burns, M. Schaeffer and W. J. Koros, *J. Appl. Polym. Sci.*, 2002, **86**, 881-890.
98. T. T. Moore, R. Mahajan, D. Q. Vu and W. J. Koros, *Aiche J.*, 2004, **50**, 311-321.
99. M. J. C. Ordonez, K. J. Balkus, J. P. Ferraris and I. H. Musselman, *J. Membr. Sci.*, 2010, **361**, 28-37.
100. Q. L. Song, S. K. Nataraj, M. V. Roussenova, J. C. Tan, D. J. Hughes, W. Li, P. Bourgoin, M. A. Alam, A. K. Cheetham, S. A. Al-Muhtaseb and E. Sivaniah, *Energy Environ. Sci.*, 2012, **5**, 8359-8369.
101. J. A. Thompson, K. W. Chapman, W. J. Koros, C. W. Jones and S. Nair, *Microporous Mesoporous Mater.*, 2012, **158**, 292-299.
102. T. X. Yang, Y. C. Xiao and T. S. Chung, *Energy Environ. Sci.*, 2011, **4**, 4171-4180.
103. T. X. Yang, G. M. Shi and T. S. Chung, *Adv. Energy Mater.*, 2012, **2**, 1358-1367.
104. T. Yang and T. S. Chung, *Int. J. Hydrog. Energy*, 2013, **38**, 229-239.
105. K. Diaz, L. Garrido, M. Lopez-Gonzalez, L. F. del Castillo and E. Riande, *Macromolecules*, 2010, **43**, 316-325.
106. K. Diaz, M. Lopez-Gonzalez, L. F. del Castillo and E. Riande, *J. Membr. Sci.*, 2011, **383**, 206-213.
107. M. Askari and T. S. Chung, *J. Membr. Sci.*, 2013, **444**, 173-183.
108. R. P. Lively, M. E. Dose, L. R. Xu, J. T. Vaughn, J. R. Johnson, J. A. Thompson, K. Zhang, M. E. Lydon, J. S. Lee, L. Liu, Z. S. Hu, O. Karvan, M. J. Realff and W. J. Koros, *J. Membr. Sci.*, 2012, **423**, 302-313.
109. C. Zhang, Y. Dai, J. R. Johnson, O. Karvan and W. J. Koros, *J. Membr. Sci.*, 2012, **389**, 34-42.
110. T. H. Bae, J. S. Lee, W. L. Qiu, W. J. Koros, C. W. Jones and S. Nair, *Angew. Chem. Int. Edit.*, 2010, **49**, 9863-9866.
111. T. X. Yang and T. S. Chung, *J. Mater. Chem. A*, 2013, **1**, 6081-6090.
112. T. Li, Y. C. Pan, K. V. Peinemann and Z. P. Lai, *J. Membr. Sci.*, 2013, **425**, 235-242.
113. S. N. Wijenayake, N. P. Panapitiya, S. H. Versteeg, C. N. Nguyen, S. Goel, K. J. Balkus, I. H. Musselman and J. P. Ferraris, *Ind. Eng. Chem. Res.*, 2013, **52**, 6991-7001.
114. X. L. Liu, Y. S. Li, G. Q. Zhu, Y. J. Ban, L. Y. Xu and W. S. Yang, *Angew. Chem. Int. Edit.*, 2011, **50**, 10636-10639.
115. X. L. Liu, Y. S. Li, Y. J. Ban, Y. Peng, H. Jin, H. Bux, L. Y. Xu, J. Caro and W. S. Yang, *Chem. Commun.*, 2013, **49**, 9140-9142.
116. X. L. Liu, H. Jin, Y. S. Li, H. Bux, Z. Y. Hu, Y. J. Ban and W. S. Yang, *J. Membr. Sci.*, 2013, **428**, 498-506.
117. G. M. Shi, T. X. Yang and T. S. Chung, *J. Membr. Sci.*, 2012, **415**, 577-586.
118. G. M. Shi, H. M. Chen, Y. C. Jean and T. S. Chung, *Polymer*, 2013, **54**, 774-783.
119. C. H. Kang, Y. F. Lin, Y. S. Huang, K. L. Tung, K. S. Chang, J. T. Chen, W. S. Hung, K. R. Lee and J. Y. Lai, *J. Membr. Sci.*, 2013, **438**, 105-111.
120. S. N. Liu, G. P. Liu, X. H. Zhao and W. Q. Jin, *J. Membr. Sci.*, 2013, **446**, 181-188.

121. D. Hua, Y. K. Ong, Y. Wang, T. X. Yang and T. S. Chung, *J. Membr. Sci.*, 2014, **453**, 155-167.
122. Y. Dai, J. R. Johnson, O. Karvan, D. S. Sholl and W. J. Koros, *J. Membr. Sci.*, 2012, **401**, 76-82.
123. P. M. Budd, E. S. Elabas, B. S. Ghanem, S. Makhseed, N. B. McKeown, K. J. Msayib, C. E. Tattershall and D. Wang, *Adv. Mater.*, 2004, **16**, 456-459.
124. A. F. Bushell, M. P. Attfield, C. R. Mason, P. M. Budd, Y. Yampolskii, L. Starannikova, A. Rebrov, F. Bazzarelli, P. Bernardo, J. C. Jansen, M. Lanc, K. Friess, V. Shantarovich, V. Gustov and V. Isaeva, *J. Membr. Sci.*, 2013, **427**, 48-62.
125. L. Hao, P. Li, T. X. Yang and T. S. Chung, *J. Membr. Sci.*, 2013, **436**, 221-231.
126. S. Basu, A. Cano-Odena and I. F. J. Vankelecom, *Sep. Purif. Technol.*, 2011, **81**, 31-40.
127. A. Demessence, C. Boissiere, D. Grosso, P. Horcajada, C. Serre, G. Ferey, G. Soler-Illia and C. Sanchez, *J. Mater. Chem.*, 2010, **20**, 7676-7681.
128. P. Kusgens, M. Rose, I. Senkovska, H. Frode, A. Henschel, S. Siegle and S. Kaskel, *Microporous Mesoporous Mater.*, 2009, **120**, 325-330.
129. G. Lu and J. T. Hupp, *J. Am. Chem. Soc.*, 2010, **132**, 7832-7833.
130. G. Lu, O. K. Farha, W. N. Zhang, F. W. Huo and J. T. Hupp, *Adv. Mater.*, 2012, **24**, 3970-3974.
131. C. Dimitrakakis, B. Marmiroli, H. Amenitsch, L. Malfatti, P. Innocenzi, G. Grenci, L. Vaccari, A. J. Hill, B. P. Ladewig, M. R. Hill and P. Falcaro, *Chem. Commun.*, 2012, **48**, 7483-7485.
132. S. Eslava, L. P. Zhang, S. Esconjauregui, J. W. Yang, K. Vanstreels, M. R. Baklanov and E. Saiz, *Chem. Mater.*, 2013, **25**, 27-33.
133. C. Zhang, R. P. Lively, K. Zhang, J. R. Johnson, O. Karvan and W. J. Koros, *J. Phys. Chem. Lett.*, 2012, **3**, 2130-2134.
134. A. W. Thornton, D. Dubbeldam, M. S. Liu, B. P. Ladewig, A. J. Hill and M. R. Hill, *Energy Environ. Sci.*, 2012, **5**, 7637-7646.
135. M. He, J. F. Yao, Q. Liu, Z. X. Zhong and H. T. Wang, *Dalton Trans.*, 2013, **42**, 16608-16613.
136. Q. Liu, Z. X. Low, L. X. Li, A. Razmjou, K. Wang, J. F. Yao and H. T. Wang, *J. Mater. Chem. A*, 2013, **1**, 11563-11569.
137. R. Molinari, L. Palmisano, E. Drioli and M. Schiavello, *J. Membr. Sci.*, 2002, **206**, 399-415.
138. P. Le-Clech, E. K. Lee and V. Chen, *Water Research*, 2006, **40**, 323-330.
139. Z. Q. Hu, Y. F. Chen and J. W. Jiang, *J. Chem. Phys.*, 2011, **134**, 134705
140. D. Li and H. T. Wang, *J. Mater. Chem.*, 2010, **20**, 4551-4566.
141. R. Z. Chen, J. F. Yao, Q. F. Gu, S. Smeets, C. Baerlocher, H. X. Gu, D. R. Zhu, W. Morris, O. M. Yaghi and H. T. Wang, *Chem. Commun.*, 2013, **49**, 9500-9502.
142. H. K. Jeong, W. Krych, H. Ramanan, S. Nair, E. Marand and M. Tsapatsis, *Chem. Mater.*, 2004, **16**, 3838-3845.
143. K. Varoon, X. Y. Zhang, B. Elyassi, D. D. Brewer, M. Gettel, S. Kumar, J. A. Lee, S. Maheshwari, A. Mittal, C. Y. Sung, M. Cococcioni, L. F. Francis, A. V. McCormick, K. A. Mkhoyan and M. Tsapatsis, *Science*, 2011, **334**, 72-75.
144. J. Choi, H. K. Jeong, M. A. Snyder, J. A. Stoeger, R. I. Masel and M. Tsapatsis, *Science*, 2009, **325**, 590-593.

TOC

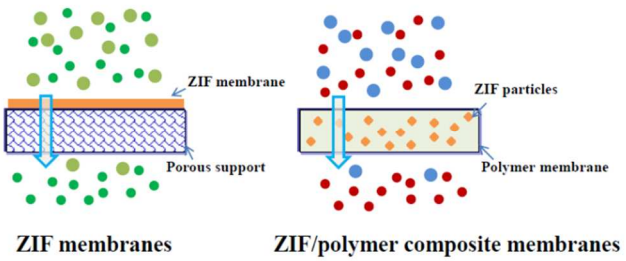

This journal is © The Royal Society of Chemistry [year]

BIOGRAPHY

Dr. Jianfeng Yao

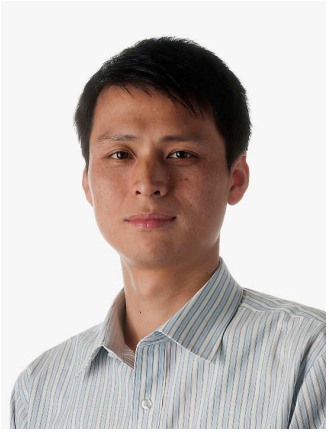

Jianfeng Yao currently is a Monash Fellow in the Department of Chemical Engineering at Monash University in Australia. He received his BE and PhD in Chemical Engineering from Nanjing University of Technology in China in 2000 and 2005, respectively. His research focuses on the preparation of porous materials, such as zeolites, metal-organic frameworks, porous carbons and titania, as well as their applications as adsorbents, catalysts and separation membranes.

Prof. Huanting Wang

Huanting Wang is a Professor in the Department of Chemical Engineering at Monash University, Australia. He received his PhD in materials science and engineering from the University of Science and Technology of China in 1997, and undertook a postdoctoral research fellowship in chemical engineering at California Institute of Technology from 1998 to 2000 and at the University of California, Riverside from 2000 to 2002. He was awarded an ARC QEII Fellowship in 2004 and an ARC future fellowship in 2010. His current research focuses on the development of nanostructured materials and membranes for gas separation, fuel cells and water treatment.